

On the Need for a Classification System for Consistent Characterization of the Composition of Planetary Bodies

David G. Russell

Owego Free Academy, 1 Sheldon Guile Blvd, Owego, NY USA

Email: russelld@oacsd.org

Abstract

A classification system is presented for characterizing the composition of planetary bodies. From mass-radius and mass-density relationships, planets may be broadly grouped into five composition classes identified as: Gas Giant, Rock-Ice Giant, gas-rich Terrestrial, Rock Terrestrial, and Rock-Ice Terrestrial based upon the mass fractions of H-He gas, rock, and ice. For each of these broad composition classes, specific bulk composition classes are defined and characterized with Solar System analog names. The classification system allows for both general and detailed characterization of exoplanets based upon planetary mass-radius-composition models and provides rationale for distinguishing “gas-rich super-Earths” from “mini-Neptunes”.

Keywords: planets and satellites: composition, terrestrial, gas giant, ice giant, brown dwarf

1 Introduction

To date over 5000 exoplanets have been confirmed (NASA Exoplanet Archive – Akeson et al. 2013). One important goal of exoplanetary research is to characterize the composition and structure of these exoplanets. For planets with accurate mass and radius measurements it is possible to determine the bulk density and, using mass-radius-composition models, describe plausible bulk compositions (e.g. Grasset et al. 2009; Lopez&Fortney 2014; Zeng et al. 2016, 2019; Aguichine et al. 2021). In addition, laboratory studies have improved the equation of state (EoS) models used for developing interior structure models (Zeng & Sasselov 2013; Hakim et al. 2018a; Helled 2018; Miozzi et al. 2018; Helled et al. 2019; Helled & Fortney 2020; Huang et al. 2021; Vazan et al. 2022) and estimating the core mass fraction (Zeng et al. 2016). Since planetary composition and structure are affected by the composition of planetary building blocks, studies of stellar abundance ratios provide valuable information for refining models of bulk composition and interior structure (Fortney 2012; Santos et al. 2017; Dorn et al. 2015, 2017; Wang et al. 2018, 2019; Bitsch & Battistini 2020; Adibekyan et al. 2021).

Despite improvement in data, characterizing planetary composition and structure is still a problem that suffers from model degeneracy and model assumptions (Dorn et al. 2017). While degeneracy is most significant in the “Neptune” and “sub-Neptune” class of planets (Wolfgang & Lopez 2015; Lozovsky et al. 2018; Jontof-Hutter 2019; Bean et al. 2021; Vazan et al. 2022), degeneracy problems persist in characterizing the mineralogy of “Earth-like” terrestrial planets (Dorn et al. 2015; Hakim et al. 2018a).

Analysis of the mass-radius (M-R) and mass-density (M- ρ) relationships for the exoplanet population indicates the existence of several break points that divide the planetary population into mass ranges with a narrower set of planetary compositions (Hatzes & Rauer 2015; Chen & Kipping 2017; Bashi et al. 2017; Fulton et al. 2017; Otegi et al. 2020). M-R and M- ρ relationships indicate that the population of planets with structure dominated by gravitational self-compression of H and He gas (gas giants) begins at approximately 120 M_{\oplus} and extends to roughly 60 Jupiter masses (M_J) (Hatzes & Rauer 2015; Chen & Kipping 2017; Bashi et al. 2017). Planets with masses from 5 to 120 M_{\oplus} include a mix of lower mass gas giants, Neptune-like planets with a rock or rock-ice interior and large H-He envelope, terrestrial planets, and rock or rock-ice composition planets with a small percentage by mass H-He envelope (Lopez & Fortney 2014; Chen & Kipping 2017; Zeng et al. 2019; Otegi et al. 2020; Owen et al. 2020), or alternatively a massive steam envelope (Turbet et al. 2020; Mousis et al. 2020; Aguichine et al. 2021). Planets with mass less than

approximately $5 M_{\oplus}$ are less likely to both accrete and maintain a significant H-He envelope and will more often have a rock or rock-ice composition (Otegi et al. 2020).

The break points identified from M-R and M- ρ relationships help to narrow the range of composition types within each mass range, but an overlap of composition types remains. For example, the rocky planet population appears to overlap the “Neptune” planet range from about 5 to $26 M_{\oplus}$ (Otegi et al. 2020) whereas the gas giant and “Neptune” populations overlap from 50 to $100 M_{\oplus}$ (Petigura et al. 2017; Otegi et al. 2020; Millholland et al. 2020).

While it appears that all planets and brown dwarfs from approximately 0.4 to $60 M_{\text{Jup}}$ have an H-He dominated composition, the primary formation mechanism may shift at different mass points within the mass range (Ma & Ge 2014; Santos et al. 2017; Narang et al. 2018; Schlaufman 2018; Goda & Matsuo 2019). Schlaufman (2018) found that core accretion is likely to be the primary formation mechanism for gas giants with masses less than $4 M_{\text{Jup}}$ whereas disk instability appears to be a more prevalent formation mechanism at masses greater than $10 M_{\text{Jup}}$. However, Adibekayn (2019) did not find evidence for a break point in formation mechanisms at $4M_{\text{Jup}}$ instead finding that environmental conditions (disk mass, metallicity) may play a larger role in formation channels. In addition, brown dwarfs, formed by star-like gas collapse (Kumar 1963), may have masses as small as 4 to $5 M_{\text{Jup}}$ (Caballero 2018; Luhman & Hapich 2020) but determining the specific formation mechanism for individual super-Jupiter mass gas giants and brown dwarfs remains problematic (Chabrier et al. 2014).

The Terrestrial planet class has a large range of possible compositions including silicate dominated (Earth), metal dominated (Mercury), carbon enriched (Bond et al. 2010; Hakim et al. 2018; Miozzi et al. 2018; Hakim et al. 2019a,b; Allen-Sutter et al. 2020), and “ocean worlds” with varying fractions of rock and ice (e.g. Europa vs. Ganymede; Grasset et al. 2009; Jontof-Hutter 2019; Bean et al. 2021). In addition, the specific mineralogy of individual terrestrial planets may vary depending upon stellar abundance ratios (Dorn et al. 2015, 2017; Santos et al. 2017; Wang et al. 2018; Adibekyan et al. 2021).

Given the large variety of planetary compositions and formation mechanisms, the degeneracy in determining interior structure and bulk composition, and overlapping mass ranges for different composition classes, characterizing exoplanet composition classes in a consistent way has been challenging. For example, Hatzes & Rauer (2015) designated planets with masses from 0.3 to $60 M_{\text{Jup}}$ as “giant planets” and planets with masses $< 0.3 M_{\text{Jup}}$ as “low mass planets” whereas Bashi et al. (2017) used the terms “small planets” and “large planets” to describe the same two populations. Goda & Matsuo (2019) suggested the giant planet population from 0.3 to $60 M_{\text{J}}$ should be divided into three mass ranges identified as “intermediate-mass planets” (0.3 - $4 M_{\text{Jup}}$), “massive planets” (4 - $25 M_{\text{Jup}}$) and “brown dwarfs” ($>25 M_{\text{Jup}}$). Chen & Kipping (2017) identified the giant planets as “Jovian” worlds and split the low mass planets into two groups: “Neptunian worlds” and “Terran worlds”. Zeng et al. (2019) used four radius ranges to divide the planetary population into “Rocky worlds”, “Water worlds”, “Transitional planets”, and “Gas giants”.

While the categorization of exoplanets is varied in the literature, the terminology suggested by Chen & Kipping (2017) closely aligns with the three broad classes of planets found in the solar system: gas giants (Jovian), ice giants (Neptunian), and terrestrial (Terran). However, the planetary population within the “Neptunian” composition mass range also includes “Terran” and “Jovian” planets (see samples and analysis in Otegi et al. 2020; Millholland et al. 2020). In addition, while Neptune-like planets are often characterized as “ice giants” it is possible that Neptune and Uranus could be rock dominated by mass, rather than ice dominated, or a “rock giant” composition (Helled et al. 2019; Helled & Fortney 2020; Teanby et al. 2020). Some Neptunian worlds may consist of a nearly pure rock body with just a small percentage by mass H-He envelope (Lopez & Fortney 2014; Zeng et al. 2019; Owen et al. 2020; Millholland et al. 2020; Bean et al. 2021) – a class of planet not found in the Solar System.

Complicating the characterization and communication of exoplanet discoveries is the use of terms such as “super-Earth”, “super-Mercury”, “super-Ganymede”, “sub-Neptune”, “super-Neptune”, and “sub-Saturn” that are applied to exoplanets which often have a mass, radius, structure, composition, or stellar flux significantly different from the Solar System bodies they are compared with. The designation of a planet as a “sub-” or “super-” Earth, Neptune, or Saturn is further complicated by the fact that these designations may be applied based upon mass, radius, or composition –

each of which can lead to a different class for the same planet. For example, a recent analysis of “sub-Saturns”, identified as planets with radius from 4.0 to 8.0 R_{\oplus} , included planets with mass ranging from 3.9 M_{\oplus} to 59.4 M_{\oplus} (Millholland et al. 2020 – hereafter MPB20). In terms of radius, planets in the MPB20 sample are “sub-Saturns”. However, in terms of mass, the sample ranges from “super-Earth” to “sub-Saturn mass” with roughly half the sample in a “Neptune” mass range of 10-30 M_{\oplus} . The envelope fractions determined in the MPB20 analysis revealed that these “sub-Saturn” radius planets can be characterized, by mass and composition, as “sub-Neptunes”, “Neptunes”, and “super-Neptunes”, but with no actual “mini-gas giants” or “Saturn” composition planets. As an extreme example, the planet Kepler 87c is a super-Earth mass (6.4 +/- 0.8 M_{\oplus}), sub-Saturn radius planet (6.14 +/- 0.29 R_{\oplus}), with a Neptune composition MPB20.

The discussion above highlights the need for a consistent classification system for characterizing and communicating the composition of planetary bodies. An example of such a composition classification system is presented in this paper. The system includes familiar terminology for five broad composition classes and Solar System analog names for characterizing possible bulk compositions within each of the broad composition classes. The goal is to provide a classification system that is flexible enough to serve as a framework for communicating planetary science discoveries to professionals, students, and the public without becoming outdated as new discoveries are made. The paper is organized as follows: General definitions related to planet classification and composition are discussed in section 2. The five broad composition classes are described in section 3. Mass ranges for the composition classes are discussed in section 4. Solar System analog names for describing bulk composition classes are described in section 5. Section 6 is the discussion and section 7 provides a conclusion.

2 Definitions

~2.1 Planetary composition components

Three types of materials provide the building blocks for planetary bodies and are identified as “rock”, “ice”, and “gas” (Stern & Levison 2002; dePater & Lissauer 2015). Depending upon planetary mass, formation history, and post formation evolution, individual planets may have significant mass fractions of one, two, or all three of these composition components:

Rock: Rock is primarily composed of the elements Mg, Si, O, and Fe (Baraffe et al. 2014). Pure rock planets will frequently have silicate minerals differentiated into a crust and mantle with an iron-rich metal alloy core. Silicate mineralogy and iron core mass fraction can vary with the abundance of elements such as Ca, Mg, Na, Al, Ni, and Fe (Dorn et al. 2017; Unterborn et al. 2017; Santos et al. 2017; Adibekyan et al. 2021). Some rock planets may be enriched in carbon and have a graphite crust (Bond et al. 2010; Hakim et al. 2019a,b).

Ice: The elements carbon, nitrogen, hydrogen, oxygen, and sulfur form molecules such as H₂O, H₂S, CH₄, NH₃, CO, N₂, and CO₂ that are collectively referred to as ‘astrophysical’ or ‘planetary’ ices. (Stern & Levison 2002; Baraffe et al. 2014; de Pater & Lissauer 2015). Due to planetary formation mechanisms (see review by Raymond et al. 2018), pure ice composition planets should be rare. Most small ice-rich Dwarf planets and Satellite planets will have a rock composition core with overlying ice and interior ocean layers (dePater & Lissauer 2015). For planets >~1 Earth mass rock and ice may have >99% miscibility in the interior and therefore fully mixed rock-ice interiors with density gradients are possible (Vazan et al. 2022).

Gas: The elements H and He are “gas” and are the main mass component of stars, brown dwarfs, and gas giant planets (Baraffe et al. 2010).

It is important to emphasize that the terms “rock”, “ice”, and “gas”, as described above, indicate composition only and do not require that the rock, ice, or gas exist in a specific state (solid, liquid, gas). Planetary interior structure models indicate that rock, ice, and gas can exist in multiple states within the same planet (e.g. dePater & Lissauer 2015) and models for different planet compositions are continuously revised as data and EoS models improve (Wahl et al. 2017; Hakim et al. 2018a, 2019a; Miozzi et al. 2018; Mazevet et al. 2019; Turbet et al. 2020; Vazan et al. 2022; Aguchine et al. 2021; Huang et al. 2021).

~2.2 Formation mechanisms and Dynamical planet classes

Spherical bodies below the hydrogen burning mass limit, about $80 M_J$, have multiple formation mechanisms and dynamical circumstances. The planetary bodies of the Solar System and most exoplanetary systems formed from materials in a circumstellar proto-planetary disk (see Raymond et al. 2018 for a review). In addition to bodies meeting the IAU definitions for “Planet” and “Dwarf Planet”, the population of spherical sub-stellar bodies also includes spherical moons such as the Moon, Ganymede, Callisto, Europa, Io, Titan, Triton, and Charon that orbit planets and dwarf planets. These bodies are “Satellite Planets” – a term that distinguishes these terrestrial bodies from the numerous smaller non-spherical moons with radius less than approximately 200 km. (Stern et al. 2015; Russell 2017). Some ice-rich exoplanets may be scaled up versions of Ganymede (Sotin et al. 2010) or “super-Ganymedes” (Jontof-Hutter 2019). It is possible that Satellite Planets orbiting exoplanets may soon be detectable (Kipping 2021).

Gas giants have three likely formation mechanisms: core accretion, disk instability, and star-like gas collapse. The core accretion and disk instability mechanisms operate in a proto-planetary disk (Boss 2001, 2003; Raymond et al. 2018; Mercer & Stamatellos 2020). Kumar (1963) proposed that the star-like gas fragmentation and collapse of molecular clouds can form bodies below the hydrogen burning mass limit. These bodies are identified as “brown dwarfs”.

3 Generalized Planetary Composition Classes

The mass-radius relationship suggests the planetary population has three broadly defined composition classes (Chen & Kipping 2017; Otegi et al. 2020): (1) Planets composed of $>50\%$ H-He gas by mass with a $<50\%$ by mass fraction of rock and ice, (2) Planets composed of $>50\%$ rock or mixed rock-ice by mass with an H-He envelope that is less than 50% by mass, and (3) Planets composed entirely of rock or mixed rock-ice with no H-He envelope. In the Solar System, these three classes are represented by Gas Giants, Ice Giants, and Terrestrial planets respectively. In this section, it is argued that each Solar System planet and all exoplanets may be assigned one of five broad composition classes identified as ***Gas Giant, Rock-Ice Giant, gas-rich Terrestrial, Rock Terrestrial, and Rock-Ice Terrestrial*** with the defining characteristics for each class accommodating a wider range of compositions and conditions than found in the Solar System (Table 1). Each of these general composition classes has multiple bulk composition classes that can be characterized with Solar System analog names as will be described in section 5.

~3.1 Gas Giant Planets and Brown dwarfs

Gas Giants include planets formed in a proto-planetary disk by core accretion or disk instability mechanisms and brown dwarfs formed by star-like gas collapse. These bodies have an H-He mass percentage greater than 50% by mass (Table 1). The Solar System’s Gas Giants, Jupiter and Saturn, most likely formed via core accretion (Raymond et al. 2018). However, the Gas Giant population with masses exceeding $4 M_{Jup}$ includes planets that may have formed by core accretion, but also formed by disk instability (Santos et al. 2017; Schlaufmann 2018; Adibekyan 2019; Goda & Matsuo 2019) and brown dwarfs formed through star-like gas collapse (Hatzes & Rauer 2015; Caballero 2018; Goda & Matsuo 2019; Luhman & Hapich 2020).

The $M-\rho$ relationship suggests that sub-stellar gas giants over the mass range 0.3 to $60 M_{Jup}$ follow the same physical relationships whether they formed by core accretion, disk instability, or star-like gas collapse (Hatzes & Rauer 2015). Importantly, it has been noted that there is no breakpoint in the $M-\rho$ relationship at $13 M_{Jup}$ that would indicate deuterium burning has a significant role in the structure and evolution of gas giant planets and brown dwarfs (Chabrier et al. 2014; Hatzes & Rauer 2015). In addition, star-like gas collapse may form bodies smaller than the deuterium burning limit (e.g. Caballero 2018; Luhman & Hapich 2020). Despite having different formation mechanisms, planets and brown dwarfs from 0.3 to $60 M_{Jup}$ all appear to share a similar structure and composition (Hatzes & Rauer 2015) and therefore “***Gas Giant***” is an appropriate general composition class for all bodies in this mass range regardless of formation mechanism.

Table 1: Generalized Planetary Composition Classes

Composition class	$f_{\text{H-He}}$ (%)	$f_{\text{rock-ice}}$ (%)	Mass Range (M_{\oplus})	Radius Range (R_{\oplus})
Gas Giant	50.1 – 100.0	0.0 – 49.9	50 – 19000	>8.1
Rock-Ice Giant	1.0 – 49.9	50.1 – 99.0	5 – 106	2.3 – 11.3
Gas-rich Terrestrial	0.01 – 0.99	99.01 – 99.99	4 - 26	1.7 – 2.8
Rock Terrestrial	<0.01	99.99 – 100.00	<11	<1.9
Rock-Ice Terrestrial	<0.01	99.99 – 100.00	<11	<2.4

~3.2 Rock-Ice Giant Planets

Models of the Solar System’s Ice Giants, Uranus and Neptune, suggest a possible composition that is ~75-90% rock and ice with the remaining 10-25% of the planetary mass in an outer H-He envelope (dePater & Lissauer 2015; Helled & Fortney 2020). Determination of the mass percentage of water and rock in these planets is difficult due to model degeneracy (Helled & Fortney 2020). The term “ice giant” is derived from models for Uranus and Neptune in which the planetary composition is >50% and possibly as large as 80% ices by mass (dePater & Lissauer 2015, Helled et al. 2020). While there are strong arguments for a significant water ice contribution to the composition of the Solar System’s ice giants, the observed parameters of Uranus and Neptune do not exclude models with a rock dominated rather than an ice dominated interior (Teanby et al. 2019; Helled et al. 2020).

Model degeneracy and the large variation in the H-He fraction (e.g. MPB20) of super-Earth to super-Neptune mass exoplanets further complicates the characterization of this class of planets. While some Neptunian planets may have a classic “ice giant” composition, numerous sub-Neptunes can be modeled as rock planets with negligible ices and a radius inflated by an H-He envelope (Lopez & Fortney 2014; Zeng et al. 2019). Planets with this composition can be described as “rock giants” rather than “ice giants” (Teanby et al. 2019; Helled et al. 2020). It has also been shown that the large radii of some “Neptunes” could be explained if Rock-Ice Terrestrial composition planets are inflated with a supercritical steam envelope (Mousis et al. 2020; Aguichine et al. 2021).

The “Neptunian” and “sub-Neptunian” radius planet population is likely to have the following general compositions: (1) a >50% by mass pure rock composition core with a negligible ice mass fraction and the remaining mass in an H-He envelope; (2) a >50% by mass mixed rock-ice core with f_{rock} greater than f_{ice} and the remaining mass in an H-He envelope; (3) a >50% by mass mixed rock-ice core with f_{ice} greater than f_{rock} and the remaining mass in an H-He envelope; and (4) a 100% rock-ice planet with no H-He envelope, but a large radius resulting from a massive supercritical steam envelope that significantly inflates the planetary radius above the pure water composition line (Mousis et al. 2020; Aguichine et al. 2021). This last composition should be grouped with the Terrestrial composition planet classes (section 3.4).

Vazan et al. (2022) found that rock and ice are potentially over 99% miscible in the interiors of planets with masses larger than approximately 1 M_{\oplus} . Planets with a bulk composition of mixed rock-ice or rock-ice-gas will not necessarily have distinct rock and ice layers. Instead, these planets could have an interior that is a rock-ice mixture with density gradients and <1% of the planetary mass in the form of an outer water layer or steam atmosphere (Vazan et al. 2022). Given the range of plausible compositions for “Neptunes” and the possibility for high miscibility of rock and ice in the interior of sub-Neptune and Neptune radius planets (Vazan et al. 2022), this class of planets can be comprehensively identified as “**Rock-Ice Giants**” rather than “Ice Giants”. The class “**Rock-Ice Giant**” indicates a rock or rock-ice planet with a 1.0 – 49.9% by mass H-He envelope (see Table 1 and section 3.4).

~3.3 Rock Terrestrial and Rock-Ice Terrestrial Planets

“Terrestrial” planets have either a 100% rock composition (Rock Terrestrial) or a 100% rock and ice composition (Rock-Ice Terrestrial). The Solar System has four Rock Terrestrial Planets with structure that includes a silicate crust, a silicate mantle, and an iron alloy core (dePater & Lissauer 2015, Zeng et al. 2016). Among the Satellite Planets in the Solar System, the Moon and Io have a Rock Terrestrial composition. The remaining Satellite Planets and most Dwarf Planets have a Rock-Ice Terrestrial composition. Vazan et al. (2022) found that the Solar System’s rock-ice

Satellite Planets have insufficient mass for rock and ice to become fully miscible in the interior. These bodies are therefore expected to have an outer icy shell and, depending upon the H₂O and Fe fractions, may have interior liquid ocean, solid ice mantle, rock mantle, and iron core layers (Schubert et al. 2010; de Pater & Lissauer 2015).

~3.4 Defining the boundary between Rock-Ice Giant and gas-rich Terrestrial planets

Otegi et al. (2020 – hereafter OBH20) suggested the exoplanet population with mass less than 120 M_⊕ may be divided into rock and rock-ice planets versus planets with an H-He envelope using the pure-water composition line in the M-R and M-ρ relationships. There is significant degeneracy in characterizing planets between the pure silicate and pure water composition lines because many possible compositions are consistent with the observed planetary mass and radius. Planets with no H-He envelope falling below the pure-water composition line are Rock or Rock-Ice Terrestrial composition. However, the population of planets with mass and radius values that place them below the pure-water composition line may include planets with an Earth-like pure rock (~30% Fe and ~70% silicate minerals) composition, or mixed rock-ice composition, but with a 0.01 to 4% by mass H-He envelope that inflates the radius (Lopez & Fortney 2014; Zeng et al. 2019; Owen et al. 2020; Armstrong et al. 2020). Some of these may be considered “*gas-rich Terrestrial*” composition planets (Owen et al. 2020; Bean et al. 2021) whereas others are more consistent with a Rock-Ice Giant composition. In this section, we consider how to usefully define the difference between *Rock-Ice Giant* planets and *gas-rich Terrestrial* planets.

The primary advantage of dividing the Terrestrial planet population from Rock-Ice Giant population using the pure-water composition line on the M-R diagram is that any planet above the pure water composition line must have a massive envelope. However, modeling the composition of this envelope suffers from degeneracy as the envelope, may be composed of H-He (Lopez & Fortney 2014; Zeng et al. 2019), H-He with water (Jontoff-Hutter 2019), or a supercritical steam envelope (Mousis et al. 2020; Agüichine et al. 2021). In addition, planets lying below the pure water composition line can still have a significant H-He envelope (Lopez & Fortney 2014; Zeng et al. 2019; Armstrong et al. 2020).

As an alternative to using the pure water composition line to divide the Terrestrial and Rock-Ice Giant populations, an **H-He mass fraction of 1.0% provides a useful composition boundary for dividing Rock-Ice Giant planets from “gas-rich Terrestrial” planets**. Planets with an H-He fraction less than 1.0% are *gas-rich Terrestrial* composition whereas planets with an H-He fraction between 1.0 and 49.9% are *Rock-Ice Giant* composition. Before considering arguments in favor of using a 1.0% H-He mass fraction to divide the Rock-Ice Giant and “gas-rich Terrestrial” planet populations, it is important to note several reasons for expecting some planets with a mass and radius combination below the pure water composition line on a mass-radius diagram will have a low percentage by mass H-He envelope:

~1. Given the nature of planetary building blocks in a proto-planetary disk and planetary formation mechanisms (see review by Raymond et al. 2018), super-Earth mass pure-water composition planets are unlikely to form (Jontoff-Hutter 2019). At distances outside the snow line in a proto-planetary disk, pebbles are composed of both rock and ice (Morbidelli et al. 2015). Super-Earth mass and larger planets falling near the pure-water composition line on the M-R diagram are therefore expected to have a rock or mixed rock-ice interior with an outer H-He envelope or supercritical steam envelope that has inflated the planetary radius (Owen et al. 2020; Mousis et al. 2020; Agüichine et al. 2021; Bean et al. 2021). For example, Osborn et al. (2021) note that a gas free model for the planet TOI-755 b (M_⊕ = 4.55 +/- 0.62, R_⊕ = 2.05 +/- 0.12) requires a water mass fraction of 73 +/- 10-13 percent that is difficult to explain from a formation point of view. However, models of TOI 755 b with an H-He envelope are consistent with an H-He mass fraction of 0.1 to 1.0 percent on mixed rock-ice or pure rock cores (Osborn et al. 2021).

~2. H-He envelopes may be stripped by stellar irradiation, core powered mass loss, or giant impacts (e.g. Owen et al. 2020; Misener & Schlichting 2021; Gupta & Schlichting 2021; Ogihara et al. 2021) and therefore a planet that forms as a Rock-Ice Giant may evolve toward a rock or rock-ice Terrestrial composition through loss of a significant fraction of the initial H-He envelope (e.g. Dai et al. 2019).

~3. Planets that reach approximately $1 M_{\oplus}$ before the gas disk dissipates during planet formation can acquire a 1% by mass H-He envelope (Owen & Mohanty 2016; Owen et al. 2020).

For each of these reasons, the planet population with masses greater than approximately $1.0 M_{\oplus}$ should include some gas-rich Terrestrial planets with a low percentage by mass H-He envelope. However, there are several drawbacks to using the pure water composition line *to define* the boundary between these gas-rich Terrestrial planets and Rock-Ice Giant planets:

~Since pure-water composition planets are generally not expected to form (Jontof-Hutter 2019; Bean et al. 2020), the pure water composition line on the M-R diagram is unlikely to represent the actual composition of observed super-Earth to Neptune mass exoplanets.

~The H-He mass fraction required to account for a pure-water composition radius increases from less than 0.1% for small Terrestrial planets to over 3% at 20 to 25 Earth masses depending upon the composition of the core (Lopez & Fortney 2014; Zeng et al. 2019). As an extreme example, TOI-849 b, which has a mass of $39.09 +2.66/-2.55 M_{\oplus}$ and radius of $3.44 +0.16/-0.12 R_{\oplus}$ (Armstrong et al. 2020), lies below the pure-water composition line. Using the pure water composition criterion, TOI-849 b would be classified as a Terrestrial planet. However, TOI-849 b is likely the remnant core of a super-Neptune or Gas Giant that retains a 2.8 - 3.9% by mass H-He envelope (Armstrong et al. 2020). While TOI-849 b falls below the pure-water composition line on the M-R diagram, this planet does not have a terrestrial composition and instead matches the Rock-Ice Giant composition class.

~Planets with an H-He envelope are subject to radius inflation resulting from a young age (Lopez & Fortney 2014; Libby-Roberts et al. 2020), increasing stellar flux or equilibrium temperature (Lopez & Fortney 2014; Zeng et al. 2019), and as a result of tidal inflation (MPB20). Mechanisms that inflate the radius of a planet can result in identical composition planets falling on opposite sides of the pure water composition line. For example, a 1 Gyr age, $8.5 M_{\oplus}$ planet with a 1% by mass H-He envelope will have radii of $2.31 R_{\oplus}$ or $2.58 R_{\oplus}$ for stellar flux values of $10 F_{\oplus}$ and $1000 F_{\oplus}$ respectively (Lopez & Fortney 2014). The pure water composition radius for an $8.5 M_{\oplus}$ planet is $2.49 R_{\oplus}$ (Zeng et al. 2016) and therefore this planet would be assigned the Terrestrial composition class for a stellar flux of $10 F_{\oplus}$, or the Rock-Ice Giant composition class for a stellar flux of $1000 F_{\oplus}$.

Using models of Zeng et al. (2019), increasing the temperature of a $4.0 M_{\oplus}$ Earth-like composition planet with a 1.0% H_2 envelope from 300K to 500K would shift the composition classification from gas-rich Terrestrial to Rock-Ice Giant if the classification is based upon the radii of the pure water composition line. Another possible mechanism for this type of classification inconsistency is tidal inflation of an H-He envelope which can significantly inflate the radii of planets with orbital periods less than 12 days (see analysis and Table 3 of MPB20).

~Rock-ice Terrestrial composition planets with no H-He envelope can have a steam envelope that inflates the planetary radius above the pure water line if the water mass fraction of the planet reaches approximately 25 - 50% (Aguichine et al. 2021).

As an alternative to the pure water composition line, it is here proposed that planets with 0.01 – 0.99% by mass H-He gas be classified as **gas-rich Terrestrial** planets and planets with 1.0 – 49.9% by mass H-He gas be classified as **Rock-Ice Giants**. In contrast to the pure water composition line, defining the boundary between gas-rich Terrestrial and Rock-Ice Giant planets using a 1.0% H-He mass fraction **provides a consistent composition boundary in the classification of planets that is not altered by inflation mechanisms**.

Given model degeneracy and uncertainty in mass and radius measurements, determining the H-He fraction for individual planets close to the pure water composition line may prove difficult in some cases. Nonetheless, the difference between a Gas Giant and a Rock-Ice Giant is defined based upon the H-He mass fraction and it therefore brings consistency to also define the difference between gas-rich Terrestrial and Rock-Ice Giant planets using a specified H-He mass fraction (Table 1).

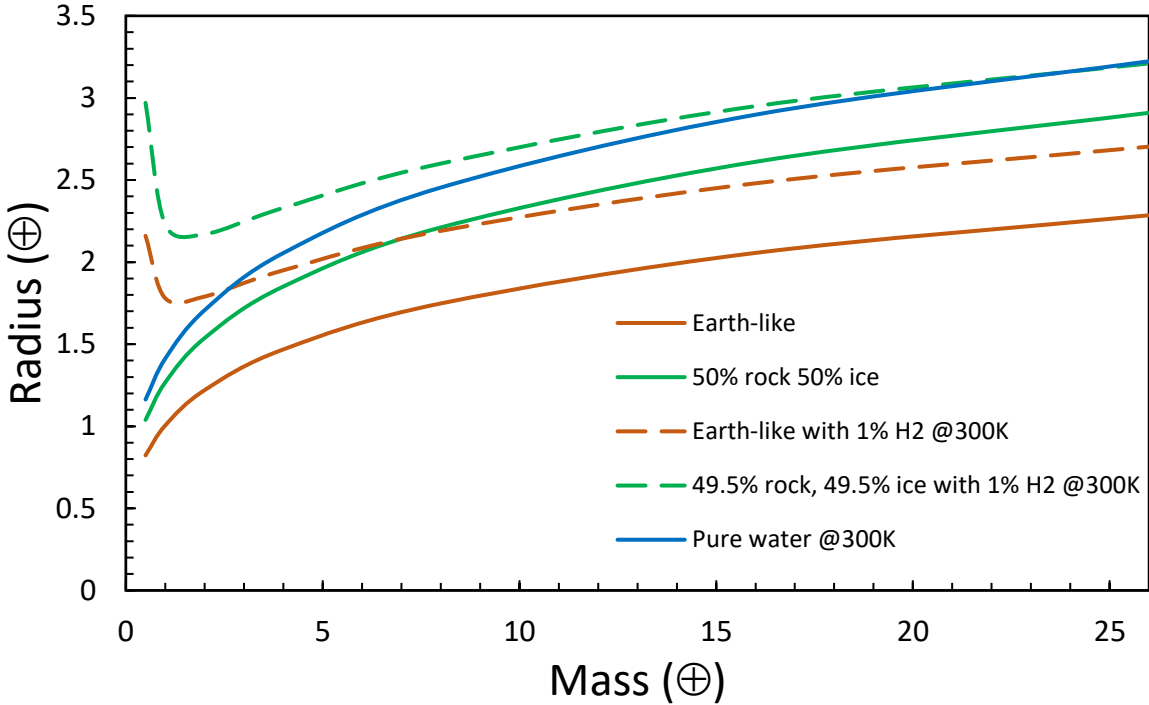


Figure 1: Mass-Radius-composition relationships for planets with mass $< 26 M_{\oplus}$ using Zeng et al. 2019 models. Composition curves shown are Earth-like (solid brown), Earth-like with 1% H_2 at 300K (dashed brown), 50% rock – 50% water (solid green), 49.5% rock and 49.5% water with 1% H_2 at 300K (dashed green), and pure water at 300K. (solid blue). In the range 7 to $26M_{\oplus}$ planets with 50% rock – 50% water to 100% water composition fall between the 300K 1% H_2 models.

The selection of 1.0% by mass as the boundary between gas-rich Terrestrial and Rock-Ice Giants is supported by the comparison of several mass-radius-composition curves in Figure 1. The solid lines in Figure 1 provide Earth-like, 50% rock – 50% water, and 100% water composition M-R curves for 0.5 to $26.0 M_{\oplus}$ planets (Zeng et al. 2016, 2019). Also plotted are 300K models for an Earth-like core with a 1.0% by mass H_2 envelope and a 49.5% rock – 49.5% water core with a 1.0% by mass H_2 envelope (Zeng et al. 2019). It is evident in Figure 1, that the 300K 1.0% H_2 envelope models reasonably bracket the envelope free 50% rock – 50% H_2O to 100% H_2O composition range. Planets that fall in this range on the M-R diagram are more likely to contain a $< 1\%$ by mass H-He envelope with a higher rock fraction than to have the envelope free high water mass fraction composition matched by their location on the M-R diagram (e.g. Osborn et al. 2021). Note that the selection of 300K models provides radii close to the minimum radii for planets with 1% by mass H-He as increasing stellar irradiation (Lopez & Fortney 2014; Zeng et al. 2019) and tidal inflation effects (MPB20) will both increase the observed planetary radii. The 300K models therefore provide radii similar to what might be expected for planets with 1% H-He by mass at greater orbital distances, or potential “cool gas-rich Terrestrial” planets.

Aguichine et al. (2021) developed M-R relationships for irradiated ocean planets using the water EoS model of Mazevet et al. (2019). These models include a refractory interior, condensed fluid H_2O layer, a steam atmosphere and no H-He envelope. Following the Aguichine et al. (2021) models, planets with a steam envelope and water mass fractions of 20% and 50% have similar radii to planets that are 50% and 100% liquid water by mass respectively in the 10-20 M_{\oplus} range.

~3.5 Summary

Every Solar System Planet, Dwarf Planet, and Satellite Planet, and all exoplanets can be assigned one of five generalized composition classes here identified as *Gas Giant*, *Rock-Ice Giant*, *gas-rich Terrestrial*, *Rock Terrestrial*, or *Rock-Ice Terrestrial*. The composition characteristics and empirical mass and radius ranges for each class are summarized in Table 1.

Each of these general composition classes has multiple possible bulk composition classes that will be described and characterized with Solar System analog names in section 5. It is important to emphasize that the composition class names do not imply that the rock, ice, and gas components must exist in specific states. Interior models are constantly changing with new analyses and equation of state models (e.g. Helled & Stevenson 2017; Hakim et al. 2018b, 2019a; Mazevet et al. 2019; Vazan et al. 2022). For example, interior models for Gas Giant and Rock-Ice Giant planets now incorporate a “fuzzy core” (e.g. Helled & Stevenson 2017; Helled et al. 2020). Recent EoS models for silicon carbide indicate that SiC is unstable in the interiors of carbon-enriched super-Earth mass planets and therefore carbon enriched exoplanets have silicate, rather than the SiC mantles found in earlier models for carbon enriched planets (Hakim et al. 2018b, 2019a). Since the broad composition classes are dependent only upon the mass fractions of H-He gas, Fe and silicate rock, and astrophysical ices, the classes will not require constant modification as new EoS and interior structure models are developed.

Section 4: Observed mass limits and overlap ranges for Terrestrial, Rock-Ice Giant, and Gas Giant composition classes

In this section, mass-radius data is examined to determine the observed upper and lower mass limits for the Rock and Rock-Ice Terrestrial, gas-rich Terrestrial, Rock-Ice Giant, and Gas Giant composition classes. The upper and lower limits also help identify the overlapping mass ranges for Terrestrial/Rock-Ice Giant and Rock-Ice Giant/Gas Giant composition classes. In order to examine this question the following samples and models are used:

- ~1. Exoplanet sample from OBH20 and references therein which includes exoplanets with mass $<120 M_{\oplus}$, mass uncertainty $<25\%$, and radius uncertainty $<8\%$.
- ~2. Confirmed exoplanets from the NASA exoplanet archive (Akeson et al. 2013) meeting the OBH20 standards for mass and radius uncertainty.
- ~3. Exoplanet sample and analysis from MPB20 which includes sub-Saturn radius (4.0 to 7.5 R_{\oplus}) planets. MPB20 provided improved H-He envelope mass fractions for the planets in their sample by accounting for tidal inflation. For planets with a gas envelope, MPB20 find that the actual envelope mass fraction at a given radius is lower in their tidal model than the envelope mass fractions determined from non-tidal models such as Lopez & Fortney (2014).
- ~4. Mass-Radius relations for Terrestrial planets with compositions ranging from pure Fe to pure H₂O (Zeng et al. 2016, 2019).
- ~5. Mass-Radius and gas envelope fraction relations developed by Lopez & Fortney (2014) and Zeng et al. (2019).
- ~6. Mass-Radius H-He envelope fraction relations for Gas Giants from Fortney et al. (2007) and Baraffe et al. (2008).

The exoplanet sample from OBH20 covers the mass range necessary to explore the upper mass limit for Terrestrial planets, the lower and upper mass limits for Rock-Ice Giants, and the lower mass limit for Gas Giants. It is important to keep in mind mass limits identified from this sample are empirical limits based upon currently known exoplanet samples with highly accurate mass and radius measurements and therefore could be adjusted with future exoplanet discoveries and reductions in mass and radius measurement uncertainty.

The upper mass limit for Gas Giants and the lower mass limit for Terrestrial planets are not covered by the OBH20 sample. For Brown dwarfs formed by star-like gas collapse mechanisms, the upper mass limit is approximately 60

M_{Jup} (Hatzes & Rauer 2015) whereas the upper mass limit for planets formed by core accretion or disk instability in a proto-planetary disk is approximately $10\text{-}25 M_{\text{Jup}}$ (Goda & Matsuo 2019).

The lowest mass Terrestrial planet in the OBH20 sample is TRAPPIST-1 d ($0.297 M_{\oplus}$). The lower mass limit for attaining a spheroidal shape, based upon the population of planetary bodies in the Solar System, is approximately 3.75×10^{19} kg, the mass of Saturn's Satellite Planet Mimas (Lineweaver & Norman 2010; Tancredi 2010; Russell 2017).

~4.1 Upper Mass Limit for Terrestrial Planets

The planets identified for the sample of OBH20 and NASA Exoplanet archive may be compared to M-R composition relationships provided by Zeng et al. (2016, 2019). The most massive planet in the OBH20 sample falling below the pure water composition line is Kepler-411 b ($M_{\oplus} = 25.76 \pm 2.544$, $R_{\oplus} = 2.40 \pm 0.056$) and sets the observed upper mass limit for the Rock Terrestrial planet class at $26 M_{\oplus}$. Using the tables for the Zeng et al. (2016, 2019) M-R relations, Kepler-411 b could have an envelope free composition that is approximately 10% Fe and 90% silicates. Given the relatively low iron fraction of this planet if it is a Rock-Terrestrial planet, Kepler-411b could instead be an Earth-like composition core gas-rich Terrestrial planet with 0.01-0.1% by mass H-He envelope (Lopez & Fortney 2014; Zeng et al. 2019).

Kepler-131b ($M_{\oplus} = 16.13 \pm 3.5$, $R_{\oplus} = 2.1 \pm 0.2/-0.1$) is another massive Rock Terrestrial or gas-rich Terrestrial planet with an H-He envelope mass fraction less than 1.0%. From Zeng et al. (2016) Kepler-131b has mass and radius that match a 20% Fe and 80% silicate minerals Rock Terrestrial planet with no H-He envelope. Following Lopez & Fortney (2014), Kepler-131b could also be a gas-rich Terrestrial planet with 30% Fe and an approximately 0.1% H-He envelope.

The five largest mass Terrestrial planets in the OBH20 sample and NASA Exoplanet Archive with radii too small to accommodate an Earth-like core gas-rich Terrestrial planet composition solution, and therefore are likely to be gas envelope free are TOI 1634 b ($10.14 \pm 0.95 M_{\oplus}$ - Hirano et al. 2021), Kepler 20b ($9.7 \pm 1.4 M_{\oplus}$), Kepler 107c ($9.39 \pm 1.77 M_{\oplus}$), HD 213885b ($8.83 \pm 0.66/-0.65 M_{\oplus}$), and K2-216b ($8.0 \pm 1.6 M_{\oplus}$). This suggests a possible upper mass limit for a pure Fe-silicate rock composition planet of $\sim 10 M_{\oplus}$. Terrestrial planets in the $10 - 26 M_{\oplus}$ mass range are more likely to be gas-rich Terrestrial planets possessing a $<1\%$ by mass H-He envelope. In the OBH20 sample, there are only seven Terrestrial composition planets with masses exceeding $10 M_{\oplus}$. Only Kepler-411 b and Kepler-131 b have radii smaller than expected for a pure-silicate rock composition supporting the possibility that most, if not all, Terrestrial planets exceeding $10 M_{\oplus}$ are gas-rich Terrestrial composition planets.

~4.2: A sample of Candidate "gas-rich Terrestrial" Composition Planets

The NASA Exoplanet Archive was searched for planets meeting the OBH20 standard for mass uncertainty ($<25\%$) and radius uncertainty ($<8\%$) to identify candidate gas-rich Terrestrial composition planets. Composition classification was determined using the mass-radius-composition models of Zeng et al (2019).

Data necessary for this classification analysis includes planetary mass, radius, and stellar flux or equilibrium temperature. The relevant models from Zeng et al. (2019) include planets with 0.1%, 0.3%, and 1% H_2 envelopes on an Earth-like core or on a 49.5% rock - 49.5% H_2O core at equilibrium temperatures of 300K, 500K, 700K, and 1000K. For a given set of mass-radius values, a gas-rich Terrestrial planet with an Earth-like core will have a higher H_2 mass fraction than a planet with a 49.5% rock - 49.5% H_2O core. Based upon the Zeng et al. (2019) models, all planets in Table 2 have $<1\%$ H_2 by mass on both rock cores and rock-ice cores. Planets that have mass-radius values consistent with $<1\%$ H_2 on a rock-ice core, but $>1\%$ H_2 on an Earth-like composition core are not included in Table 2 as any such planets are possible Rock-Ice Giants.

Table 2: Candidate gas-rich Terrestrial Planet Sample

Planet	Mass (M_{\oplus})	Radius (R_{\oplus})	S_{\oplus} / T_{eq} (K) ^a	Mass –Radius Reference
TOI-776 b	4.0 +/-0.9	1.85 +/-0.13	11.5 / 514	Luque et al. 2020
GJ 9827 d	4.04 +0.82/-0.84	2.022 +.046/-0.043	- / 646	Rice et al. 2019
Kepler 60 d	4.16 +0.84/-0.75	1.99 +/-0.16	161 / -	Jontof-Hutter et al. 2016
Kepler 60 b	4.19 +0.56/-0.52	1.71 +/-0.13	318 / -	Jontof-Hutter et al. 2016
TOI-755 b	4.55 +/-0.62	2.05 +/-0.12	731 / 1371	Osborn et al. 2021
TOI-270 d	4.78 +/-0.43	2.133 +/-0.058	- / 387	VanEylen et al. 2021
HD 39091 c	4.82 +0.86/-0.84	2.05 +/-0.50	309 / 1170	Huang et al. 2018
K2-111 b	5.29 +0.76/-0.77	1.82 +0.11/-0.09	- / 1309	Mortier et al. 2020
K2-146 b	5.77 +/-0.18	2.05 +/-0.06	20.7 / 534	Hamann et al. 2019
TOI-1201 b	6.28 +0.84/-0.88	2.415 +0.091/-0.090	40.6 / 703	Kossakowski et al. 2021
K2-138 c	6.31 +1.13/-1.23	2.299 +0.120/-0.087	249 / 1012	Lopez et al. 2019
Kepler 454 b	6.84 +/-1.40	2.37 +/- 0.13	116 / -	Gettel et al. 2016
TOI-421 b	7.17 +/-0.66	2.68 +0.19/-0.18	155 / 981	Carleo et al. 2020
Kepler 307 b	7.44 +0.91/-0.87	2.43 +/- 0.09	59.7 / -	Jontof-Hutter et al. 2016
TOI-178 f	7.72 +1.67/-1.52	2.287 +0.108/-0.110	- / 521	Leleu et al. 2021
HD 5278 b	7.8 +1.5/-1.4	2.45 +/- 0.05	132 / 943	Sozzetti et al. 2021
K2-138 d	7.92 +1.39/-1.35	2.39 +0.104/-0.084	147 / 888	Lopez et al. 2019
HD 97658 b	8.3 +/-1.1	2.12 +/-0.06	- / 751	Ellis et al. 2021
TOI-1260 b	8.60 +/-1.50	2.34 +/-0.11	91 / 860	Georgieva et al. 2021
Kepler 102 e	8.93 +/-2.0	2.22 +/-0.07	20 / -	Marcy et al. 2014
K2-285 b	9.68 +1.21/-1.37	2.59 +/-0.06	234 / 1089	Palle et al. 2019
TOI-763 b	9.79 +/-0.78	2.28 +/-0.11	- / 1038	Fridlund et al. 2020
TOI-1062 b	10.15 +0.81/-0.84	2.265 +0.96/-0.91	- / 1077	Otegi et al. 2021
Kepler 538 b	10.6 +2.5/-2.4	2.215 +0.040/-0.034	2.99 / 380	Mayo et al. 2019
K2-263 b	14.8 +/-3.1	2.41 +/-0.12	- / 470	Mortier et al. 2018
Kepler 131 b	16.13 +/-3.5	2.41 +/-0.20	66 / -	Marcy et al. 2014
HIP 97166 b	20.0 +/-1.5	2.74 +/-0.13	- / 757	MacDougall et al. 2021
GJ 143 b	22.7 +2.2/-1.9	2.61 +0.17/-0.16	- / 422	Drogomir et al. 2019
K2-292 b	24.5 +/-4.4	2.63 +0.11/-0.10	67 / 795	Luque et al. 2019
Kepler 411 b	25.6 +/-2.6	2.401 +/-0.053	- / 1138	Sun et al. 2019

Note a – stellar flux and equilibrium temperatures identified from multiple sources in the NASA Exoplanet archive.

The population of candidate gas-rich Terrestrial composition planets identified from the current exoplanet sample, meeting the OBH20 standards for mass and radius uncertainty, and with stellar flux or equilibrium temperature values available in the NASA Exoplanet Archive, has a mass range of 4.0 – 25.6 M_{\oplus} and a radius range of 1.70 to 2.75 R_{\oplus} . Many of the planets listed in Table 2 fall into a radius range often identified as “mini-Neptunes”. However, based upon the composition analysis, these planets are instead examples of “gas-rich super-Earth” composition planets. This class of planet which has a voluminous, but low percentage by mass H-He envelope on a Terrestrial core, represents the first fundamentally new type of planet that has been identified in exoplanet studies (Bean et al. 2021).

~4.3 Lower Mass Limit for Rock-Ice Giants

As defined in this paper, the H-He envelope mass fraction of a Rock-Ice Giant planet is between 1.0 and 49.9 % by mass. The lowest mass Rock-Ice Giant planets from the OBH20 sample, the MPB20 sample, and the list of confirmed planets from the NASA Exoplanet archive which meet the OBH20 standard for mass and radius uncertainty are listed in Table 3. Most of these planets have masses between 6.2 M_{\oplus} and 6.9 M_{\oplus} . The lowest mass planet that must have an H-He envelope fraction exceeding 1.0% using the Zeng et al. (2016, 2019) composition models is Kepler 26 b with a mass of 5.12 +0.65/-0.61 M_{\oplus} (Jontof-Hutter et al. 2016). The observed mass range for the lower mass limit of Rock-Ice Giant composition planets is therefore 5-7 M_{\oplus} .

Table 3: Lowest mass Rock-Ice Giants

Planet	Mass (M_{\oplus})	Radius (R_{\oplus})	Reference
Kepler 26b	5.12 +0.65/-0.61	2.78 +/-0.11	Jontof-Hutter et al. 2016
TOI-561 c	5.40 +/-0.98	2.878 +/- 0.096	Lacadelli et al. 2020
Kepler 177 b	5.84 +0.86/-0.82	3.50 +0.19/-0.15	Vissapragada et al. 2020
Kepler 26 c	6.20 +/-0.65	2.72 +/-0.12	Jontof-Hutter et al. 2016
LTT 3780 c	6.29 +0.63/-0.61	2.42 +/- 0.10	Nowak et al. 2020
Kepler 79e	6.3 +/-1.0	3.414 +/- 0.129	Yoffe et al. 2020
Kepler-87 c	6.4 +/- 0.8	6.14 +/- 0.29	Millholland et al. 2020
TOI-125 c	6.63 +/-0.99	2.759 +/-0.10	Nielsen et al. 2020
Kepler-11 e	6.7 +1.2/-1.0	4.0 +0.2/-0.3	Hadden & Lithwick 2017
Kepler 80 c	6.74 +1.23/-0.86	2.74 +/-0.12	MacDonald et al. 2016
Kepler-11 d	6.8 +0.7/-0.8	3.3 +/-0.2	Hadden & Lithwick 2017
Kepler 80 b	6.93 +1.05/-0.70	2.67 +/- 0.10	MacDonald et al. 2016
Kepler-36 c	7.13 +/-0.18	3.679 +/-0.098	Vissapragada et al. 2020
HD 191939 c	7.2 +/-1.4	3.08 +/- 0.07	Lubin et al. 2022
Kepler-223 d	8.0 +1.5/-1.3	5.24 +0.26/-0.45	Mills et al. 2016
GJ 1214 b	8.17 +/- 0.43	2.742 +/-0.05	Cloutier et al. 2021

~4.4 Upper Mass Limit for Rock-Ice Giants and Lower mass limit for Gas Giants

The tidal inflation model of MPB20 complicates determination of the upper mass limit for Rock-Ice Giants and lower mass limit for Gas Giants. The results of MPB20 demonstrate that planets with large radii consistent with an uninflated Gas Giant composition, falling at or above the 50% H-He line on the M-R diagram, can have a tidally inflated radius. Many of these tidally inflated planets will therefore actually be Rock-Ice Giant composition with an H-He mass fraction less than 50 percent. Tidal inflation has a greater impact on planets with shorter orbital periods (MPB20). Planets in the MPB20 sample with orbital periods < 12 days have H-He envelope fractions after accounting for tidal inflation that are only 25-50% of the value derived from a non-tidal model (see Table 3 of MPB20). Most planets in the OBH20 sample from 40 - 120 M_{\oplus} have orbital periods <6 days and therefore should experience H-He envelope tidal inflation.

The tidal model of MPB20 did not explore planets with actual fenv > 50%. Based upon the models of Fortney et al. (2007) and Baraffe et al. (2008), planets with 50% H-He and 90% H-He and with mass ranging from 50 – 100 M_{\oplus} should have radii of 8.1-8.3 R_{\oplus} and 11.4 R_{\oplus} respectively for a 5 Gyr and 0.045 AU model. If the results of MPB20 extrapolate to radii larger than sub-Saturn radius planets, many short orbital period planets with non-tidally inflated model gas fractions greater than 50% are likely to have actual gas mass fractions less than 50%. Any such planets would be inflated Rock-Ice Giants rather than Gas Giants. As an example, MPB20 demonstrated that WASP-107 b ($R_{\oplus} = 10.6 +/- 0.3$), which has a non-Tidal envelope fraction of approximately 75%, could have an actual envelope fraction as low as 10% after accounting for tidal inflation.

For the OBH20 sample with orbital periods <12 days, planets with radii < 9.9 R_{\oplus} , or about 60% H-He with models that do not account for tidal inflation (Fortney et al. 2007; Baraffe et al. 2008), will be considered Rock-Ice Giants. Planets with radii from 9.9 – 11.4 R_{\oplus} will be considered possible Rock-Ice Giants, and planets with radii >11.4 R_{\oplus} will be considered Gas Giants.

The most massive planet from the OBH20 sample with radius less than 8.1 R_{\oplus} , and therefore must be a Rock-Ice Giant regardless of tidal inflation effects is CoRoT-8 b ($M_{\oplus} = 69.3 +/- 10.8$; $R_{\oplus} = 6.94 +0.18 -0.19$ – Raetz et al. 2019). The most massive short orbital period planets from the OBH20 sample with radii less than 9.9 R_{\oplus} have masses from 100 - 106 M_{\oplus} (K2-287 b, HD 149026 b, and K2-295 b). The upper mass limit for Rock-Ice Giants is therefore at least 70 M_{\oplus} and likely 100-110 M_{\oplus} .

The least massive Gas Giants in the OBH20 sample with radii exceeding $11.4 R_{\oplus}$ have masses from $52 - 57 M_{\oplus}$ (HAT-P-48 b, KELT-11 b, and WASP-127 b). Therefore, the mass overlap range for Rock-Ice Giant and Gas Giant planet populations is approximately $50 - 110 M_{\oplus}$.

Section 5: Solar System Analog Names for Characterizing Planetary Bulk Composition Classes

The classes *Rock Terrestrial*, *Rock-Ice Terrestrial*, *gas-rich Terrestrial*, *Rock-Ice Giant*, and *Gas Giant* provide a broad characterization of the rock, ice, and gas composition of planets (Table 1). However, within each class there can be important differences in composition. For example, Rock Terrestrial planets can be “Earth-like” with a silicate fraction $> 50\%$ or “Mercury-like” with iron fraction $>50\%$. Rock-Ice Giants and Rock-Ice Terrestrial planets will have varying fractions of rock and ice ranging from mostly rock to mostly ice, while Gas Giants can have $Z > 2$ element fractions ranging from $<10\%$ to nearly 50% . Table 4 provides a list of planetary bulk compositions and a system Solar System analog names for characterizing the bulk composition classes. Table 5 provides examples of the Solar System analog names applied to exoplanets.

Table 4: Planet Composition Classes with Solar System Analog Names

Composition Class	$f_{\text{H-He}}$ (%)	$f_{\text{R-I}}$ (%)	Mass Range (M_{\oplus})
<i>Gas Giants</i>	50.1 - 100.0	0.0 - 49.9	50 - 19000
Brown Dwarf	90.0 - 100.0	<10.0	4100 - 19000
Super-Jupiter	90.0 - 100.0	<10.0	1300 - 4100
Jupiter	80.1 - 100.0	0.0 - 19.9	50 - 1300
Saturn	50.1 - 80.0	20.0 - 49.9	50 - 300
<i>Rock-Ice Giants</i>	1.0 - 49.9	50.1 - 99.0	5 - 110
Super-Neptune			50 - 110
Neptune			10 - 50
Sub-Neptune			5 - 10
<i>Gas-rich Terrestrial</i>	0.01 - 0.99	99.01 - 99.99	4 - 26
Gas-rich super-Mercury			
Gas-rich super-Earth			
Gas-rich super-Europa			
Gas-rich super-Ganymede			
<i>Rock-Terrestrial</i>	<0.01	>99.99	<11
Earth a			<4
Mercury b			<4
Carbon-rich Earth c			<4
Super-Earth			4 - 11
Super-Mercury			4 - 11
Carbon-rich super-Earth			4 - 11
<i>Rock-Ice Terrestrial</i>	<0.01	>99.99	<11
Ganymede d			<4
Super-Ganymede			4 - 11
Europa e			<4
Super-Europa			4 - 11

Notes: a – Earth class planets have $>50\%$ silicates and $<50\%$ iron by mass, b – Mercury class planets have $> 50\%$ iron and $< 50\%$ silicates by mass, c – carbon-rich Earth planets have a carbon saturated rock mineralogy, d – Ganymede class planets are $>10\%$ ice and $<90\%$ rock by mass, e – Europa class planets have $0.2 - 10\%$ ice and $90.0-99.8\%$ rock by mass. Rock Terrestrial planets are $<0.01\%$ H-He and $<0.2\%$ ice by mass.

~5.1 Rock, Rock-Ice, and gas-rich Terrestrial Composition Classes

Rock Terrestrial planets can be divided into three bulk composition classes which indicate rock planets that are >50% iron (Mercuries), >50% silicates (Earths), and carbon enriched (carbon-rich Earths). Earth, Mercury, and carbon-rich Earth planets are those with mass < 4 Earth masses. Rock Terrestrial planets with masses from 4 – 11 M_{\oplus} overlap the mass range for gas-rich Terrestrial planets (Section 4.2) and are characterized as super-Mercury, super-Earth, or carbon-rich super-Earth composition planets. Adibekyan (2021) has identified a list of super-Mercury class planets with >60% Fe by mass.

Carbon-rich Earth/super-Earth planets are carbon-saturated and more likely to form around stars with C/O ratios > 0.8 (Bond et al. 2010). Fortney (2012) found that 10-15% of stars may have a C/O ratio > 0.8. However, more recent studies have found 100% of stars in the samples with C/O ratios < 0.8 (Suárez-Andrés et al. 2018; Bedell 2018) indicating carbon-enriched planets could be rare. Bond et al. (2010) presented models for carbon-enriched planets as “carbide planets” with an iron-carbide alloy core, and a mantle composed of SiC and TiC overlain by a graphite crust. Allen-Sutter et al. (2020) found that delivery of water to a carbide planet could result in a silicate crust and diamond with hydrous silica overlying a mantle of SiC. However, from high temperature and pressure experiments, Hakim et al. (2018b, 2019a) found that SiC is unstable in the interiors of larger rocky exoplanets unless the conditions are extremely reducing. Hakim et al. (2019a) presented models for the interior of carbon-enriched rocky exoplanets that include a metallic iron alloy core, a silicate (pyroxene and olivine) mantle with no SiC, and a graphite crust. Once a carbon-enriched planet reaches C-saturation, additional carbon does not alter the silicate mineralogy but simply adds to the graphite crust with an increasing possibility of a diamond-silicate upper mantle (Hakim et al. 2019a).

Rock-Ice Terrestrial planets can be divided into Ganymede-like and Europa-like bulk composition classes. Ganymede composition class planets have >10% ices by mass whereas Europa composition class planets have 0.2 – 10% ices by mass. As with Rock-Terrestrial planets, super-Ganymede and super-Europa class planets overlap the gas-rich Terrestrial mass range from 4 – 11 M_{\oplus} , whereas Ganymede and Europa class planets are < 4 M_{\oplus} .

Lingam & Loeb (2019) found that in order to cover all land masses on Earth a minimum of 4.3 oceans of surface water is required – or approximately 6.3 total oceans after accounting for the Earth’s estimated mass of mantle water. Adopting 1.4×10^{21} kg per ocean indicates that an Earth-mass planet with approximately 0.15% by mass water could be an “ocean world” free of exposed land mass. Therefore, a minimum planetary water mass fraction of 0.2% is adopted for Rock-Ice Terrestrial composition planets. The bulk composition of Europa is over 90% silicates and iron but includes an ice crust and interior ocean layer with a total thickness slightly over 100 km (Vance et al. 2017). Europa class planets therefore will have 0.2 – 10% of the total planetary mass as water and other ices. Ganymede and super-Ganymede class planets have >10% ices by mass.

Gas-rich Terrestrial planets have masses ranging from 4.0 – 26.0 M_{\oplus} (section 4.2). These planets are rock or rock-ice Terrestrial composition planets with a 0.01 – 0.99 percent by mass H-He envelope. The bulk composition classes are “gas-rich super-Earth”, “gas-rich super-Mercury”, “gas-rich super-Europa”, and “gas-rich super-Ganymede”. Given model degeneracy, additional data beyond mass, radius, and equilibrium temperature (T_{eq}) will be needed to distinguish between the possible gas-rich Terrestrial bulk composition classes.

~5.2 Rock-Ice Giant composition classes

Rock-Ice Giants have H-He envelopes that account for 1.0 – 49.9 percent of the planetary mass. The cores of Rock-Ice Giants can have varying rock-ice fractions including: (1) a pure rock composition; (2) a mixed rock-ice composition with f_{rock} greater than f_{ice} ; and (3) a mixed rock-ice composition with f_{ice} greater than f_{rock} . The traditional “Ice Giant” composition models for Uranus and Neptune (dePater & Lissauer 2015) would be consistent with the third composition type. However, a “Rock Giant” composition, consistent with the first two composition types cannot be ruled out for Uranus and Neptune (Helled & Fortney 2020; Teanby et al. 2020). As an example from the exoplanet population, the planets of the TOI-125 system, TOI-125b, TOI-125c and TOI-125d, are modeled by Nielsen et al. (2020) to have 2.0 - 4.1% H-He gas, 62-70% rock, and 32-36% water which is consistent with “Rock Giant” composition.

Table 5: Composition Classification Applied to Exoplanets

Planet	Period (d)	Mass (M_{\oplus})	Radius (R_{\oplus})	Teq (K)	Reference	Classification
LHS 1140c	3.77	1.77 +.17/-0.16	1.169 +/-0.037	709	Lillo-Box et al. 2020a	Earth
GJ 486b	1.47	2.82 +0.11/-0.12	1.305 +/-0.06	701	Trifanov et al. 2021	Earth
Kepler 36 b	13.84	5.56 +0.41/-0.45	1.582 +/-0.015	978	Yofee et al. 2021	Super-Earth
K2-291 b	2.225	6.4 +/-1.1	1.582 +/-0.04		Dai et al. 2019	Super-Earth
HD213885 b	1.008	8.83 +/-0.66	1.745 +/-0.052	2128	Espinoza et al. 2020	Super-Earth
K2-229 b	0.58	2.49 +.43/-0.45	1.197 +/-0.04	1818	Dai et al. 2019	Mercury
HD 137496 b	1.62	4.04 +/-0.55	1.31 +.06/.05	2130	Azevedo Silva et al. 2022	Super-Mercury
Kepler 107 c	4.901	9.39 +/-1.77	1.597 +/-0.026	1379	Bonoma et al. 2019	Super-Mercury
L98-59 c	3.69	2.22 +0.26/-0.25	1.385 +.095/-0.075	553	Demangeon et al. 2021	Europa
HD136352 b	11.58	4.72 +/-0.42	1.664 +/-0.043	905	Delrez et al. 2021	Super-Ganymede
TOI-776 b	8.25	4.00 +/- 0.9	1.85 +/-0.13	514	Luque et al. 2021	Gas-rich super-Earth
TOI-1260 b	3.93	8.60 +/- 1.50	2.34 +/-0.11	860	Georgieva et al. 2021	Gas-rich super-Earth
HD136352 d	107.25	8.82 +/-0.9	2.562 +.09/-0.08	431	Delrez et al. 2021	Gas-Rich super-Ganymede
Kepler 538 b	81.74	10.6 +2.5/-2.4	2.215 +.04/-0.03	380	Mayo et al. 2019	Gas-rich super-Ganymede
K2-263 b	50.8	14.8 +/-3.1	2.41 +/-0.12	470	Mortier et al. 2018	Gas-rich super-Earth
Kepler 411 b	3.00	25.6 +/-2.6	2.401 +/-0.053	1138	Sun et al. 2019	Gas-rich super-Earth
TOI-561 c	10.78	5.40 +/-0.98	2.878 +/-0.096	860	Lacadelli et al. 2020	Sub-Neptune
Kepler 36 c	16.22	7.13 +/-0.18	3.679 +/-0.098	928	Vissapragada et al. 2020	Sub-Neptune
GJ 1214 b	1.58	8.17 +/-0.43	2.742 +/-0.05	596	Cloutier et al. 2021	Sub-Neptune
LTT 3780 c	12.25	8.60 +1.60/-1.30	2.30 +.16/-0.15	353	Cloutier et al. 2020	Sub-Neptune
TOI 431 d	12.46	9.90 +/-1.5	3.29 +/-0.09	633	Osborn et al. 2021	Sub-Neptune
HD 136352 c	27.59	11.24 +/-0.06	2.916 +/-0.07	677	Delrez et al. 2021	Neptune
K2-32 b	8.99	15.0 +1.8/-1.7	5.30 +/-0.19	837	Lillo-Box et al. 2020b	Neptune
GJ 436 b	2.64	23.1 +/-0.8	4.19 +/-0.109	686	Turner et al. 2016	Neptune
K2-19 b	7.92	32.4 +/-1.7	7.0 +/-0.2	854	Petigura et al. 2020	Neptune
TOI-849 b	0.77	39.09 +2.7/-2.6	3.44 +.16/-0.12		Armstrong et al. 2020	Neptune
K2-108 b	4.73	59.4 +/-4.4	5.33 +/-0.21	1446	Petigura et al. 2017	Super-Neptune
CoRot-8 b	6.21	69.3 +/-10.8	6.94 +/-0.2	870	Raetz et al. 2019	Super-Neptune
WASP-127 b	3.38	52.35 +6.8/-5.5	14.69 +/-0.3	1400	Seidel et al. 2020	Saturn
KOI-1783.01	134.46	71 +11/-9	8.86 +.25/-0.24		Vissapragada et al. 2020	Saturn
NGTS-11 b	35.46	109 +29/-23	9.16+.31/-0.36	435	Gill et al. 2020	Saturn
Kepler 539 b	125.63	308 +/-92	8.37 +/-0.19	388	Mancini et al. 2016	Saturn
TOI-1899 b	29.02	210 +/-22	12.9 +0.4/-0.6	362	Cañas et al. 2020	Jupiter
CoRoT-9 b	95.27	267 +/-16	11.95 +0.8/-0.7	420	Bonomo et al. 2017	Jupiter
Kepler 167 e	1071	321 +51/-48	10.16 +/-0.42	134	Chachan et al. 2022	Jupiter
KOI-3680 b	141.24	613 +60/-67	11.1 +0.7/-0.8	347	Hébrard et al. 2019	Jupiter
Kepler 1704 b	988.88	1319 +/-92	11.94 +.48/-0.46	254	Dalba et al. 2021	Super-Jupiter
Kepler 1514 b	217.83	1678 +/-70	12.42 +/-0.26	388	Dalba et al. 2021	Super-Jupiter

The Solar System analog names for the Rock-Ice Giant class are “Neptune”, “sub-Neptune”, or “super-Neptune”. Given the large impact from inflationary mechanisms on the radius of planets with massive H-He envelopes (e.g. Lopez & Fortney 2014; Zeng et al. 2019; Millholland et al. 2020), planetary mass provides a more reliable parameter for characterizing Rock-Ice Giants as “sub” or “super” Neptunes than planetary radius. For example, Kepler 87c is a Neptune composition planet (MPB20) with a super-Earth mass ($6.4 \pm 0.8 M_{\oplus}$) and a sub-Saturn radius ($6.14 \pm 0.29 R_{\oplus}$). Based upon the mass ranges for the composition classes identified in section 4, Kepler 87c falls into the mass range for Rock-Terrestrial planets ($<10 M_{\oplus}$) and therefore can be classified as a “sub-Neptune” despite having a radius 50% larger than Neptune. As indicated in Table 4, the mass ranges for sub-Neptune, Neptune, and super-Neptune class planets are $5\text{--}10 M_{\oplus}$, $10\text{--}50 M_{\oplus}$, and $50\text{--}110 M_{\oplus}$ respectively. The sub-Neptune mass range overlaps with the Rock-Terrestrial population mass range (sections 4.1 and 4.3) whereas the super-Neptune mass range overlaps with the Gas Giant population mass range (section 4.4).

~5.3 Gas Giant Composition Classes

Gas Giants have an H-He envelope mass fraction $>50\%$ by mass with rock-ice (metal) fractions $<50\%$ by mass. Models of Jupiter and Saturn indicate metal fractions of $<10\%$ and $20\text{--}30\%$ respectively (Helled 2018). Based upon exoplanet samples and formation mechanisms, the maximum mass of metals is expected to be in the range $50\text{--}100 M_{\oplus}$ for most Gas Giants (e.g. Fortney et al. 2007; Miller & Fortney 2011; Lambrechts et al. 2014; Mocquet et al. 2014) and therefore the metal fraction is expected to be less than 20% for most Jupiter mass and larger Gas Giants.

The Solar System analog names for Gas Giants are “Jupiter” for planets with $<20\%$ metals by mass and “Saturn” for planets with $20.0\text{--}49.9\%$ metals by mass. The mass range of Saturn and Jupiter class planets potentially overlaps from $50\text{ to }300 M_{\oplus}$. Millholland et al. (2020) found the H-He mass fraction of the super-Neptune K2-108b is only 5.9%. With a mass of $59.4 M_{\oplus}$, K2-108b would have a total metal mass of approximately $56 M_{\oplus}$ which indicates Saturn composition planets could reach at least $280 M_{\oplus}$. The upper mass limit for Saturn composition planets is therefore listed as $300 M_{\oplus}$ in Table 4. Kepler 539 b is a high mass Saturn composition planet with a mass $308 M_{\oplus}$ but a relatively large uncertainty of $\pm 92 M_{\oplus}$ (Mancini et al. 2016).

Based upon formation mechanisms, star forming gas collapse could form Brown Dwarfs as small as $\sim 4 M_{\text{Jup}}$ (Caballero 2018; Luhman & Hapich 2020) and disk instability could form Gas Giants as large as $\sim 25 M_{\text{Jup}}$ (Goda & Matsuo 2019). Following Lecavelier & Lissauer (2022), Brown Dwarfs are identified in Table 4 as Gas Giants with a mass exceeding the deuterium burning limit of approximately $13 M_{\text{Jup}}$ regardless of formation mechanism and therefore will have metal mass fractions $<10\%$. Note that if Brown Dwarfs are instead defined by formation mechanism (e.g. Chabrier et al. 2014), then the lower mass limit for the Brown dwarf composition class becomes $4 M_{\text{Jup}}$ or $\sim 1300 M_{\oplus}$ and would overlap the Jupiter composition class mass range from $4\text{--}25 M_{\text{Jup}}$.

6 Discussion

~6.1 Composition Classification as an Algorithm

Stern & Levison (2002) suggested eight criteria for an algorithm to determine the classification of a body as a “planet”. These criteria are that the definition: (1) be physically based, (2) be determined based upon observable characteristics, (3) be quantitative, (4) uniquely classify any given body, (5) be deterministic, (6) be comprised of the fewest possible criteria, (7) be robust to new discoveries, and (8) be reasonably backward compatible. While Stern & Levison (2002) proposed these criteria for an algorithm that would determine whether or not a body is a planet, it is worthwhile to note that the composition classification system described in this paper meets seven of these criteria.

The broad composition classes Rock-Terrestrial, Rock-Ice Terrestrial, gas-rich Terrestrial, Rock-Ice Giant, and Gas Giant are identified from the planetary mass fractions of H-He gas, rock and ice. This characteristic of the composition system (Table 1) meets five of the eight criteria proposed by Stern & Levison (2002). Specifically, the

composition classification system is physically based, quantitative, uniquely classifies every planet's composition, is robust to new discoveries, and comprises a small number of classification criteria.

Note that while model degeneracy and data uncertainty will in some cases make it difficult to determine which of the classes a specific exoplanet should be assigned to, each planet can only have one of the broad composition classes. Therefore the composition classification system can uniquely classify every planetary body when the necessary data is available.

The system is also robust to future discoveries in several ways. First, since the broad composition classes are based upon the mass fractions of the H-He and rock-ice components, every newly discovered exoplanet must fall into one of the five broad composition classes. Second, the bulk composition classes described provide more detailed composition characterization. If new, exotic planetary compositions are discovered, these compositions can be added to the list of bulk compositions without abandoning those classes already described or requiring new broad composition classes. The carbon-enriched terrestrial composition provides an example of this flexibility as this bulk composition class represents an exotic composition not found in the Solar System. Third, since the composition classification system is not dependent upon interior structure models the system will not require constant revisions as equation of state and interior structure models improve (e.g. Helled & Stevenson 2017; Wahl et al. 2017; Hakim 2018b, 2019a).

The composition classification system also meets the criteria of being based upon observable characteristics as determination of the composition class of a planet is primarily derived from mass and radius measurements which are analyzed in the context of mass-radius-composition models that are derived from EoS models and the planet's stellar flux.

The composition system discussed in this paper is also “backward compatible” by which Stern & Levison meant to avoid numerous reclassifications that would confuse lay people. The five broad classes place Solar System planets into the same classes they have previously been assigned to with the slight modifications being: (1) that the traditional “Ice Giants” are now “Rock-Ice Giants” as explained in section 3.2 and (2) the Terrestrial planet class is divided into Rock-Terrestrial, Rock-Ice Terrestrial, and gas-rich Terrestrial. These slight modifications maintain familiar terminology while allowing the composition classification system to meet the condition of uniquely classifying any given body.

The only criterion from the Stern & Levison (2002) list that the composition classification system does not meet is that the system cannot be deterministic, by which they argued the classification of a body as a “planet” should not change over time. This criterion cannot fully apply to planetary composition due to the volatile nature of planetary envelopes which may be stripped through core powered mass loss, photo-evaporation, and giant impacts (Owen et al. 2020; Misener & Schlichting 2021; Gupta & Schlichting 2021; Ogihara et al. 2021). Therefore, planets that start out as Gas Giants or Rock-Ice Giants can evolve to a different composition class over time if the gas envelope is sufficiently stripped (e.g. Dai et al. 2019; Armstrong et al. 2020).

~6.2 Usefulness of the Composition Classification System

The composition classification system presented in this paper has a number of useful characteristics. The five broad composition classes *Gas Giant*, *Rock-Ice Giant*, *gas-rich Terrestrial*, *Rock Terrestrial*, and *Rock-Ice Terrestrial* provide familiar terminology originating with known Solar System composition classes. However, each composition class allows for a broader range of composition characteristics than found in the planetary population of the Solar System. All Solar System planets and all exoplanets may be grouped into one of these five classes depending only upon the mass fractions of H-He gas, rock, and ice.

Modeling the composition of exoplanets suffers from degeneracy and many planets will have a mass and radius consistent with several possible bulk compositions. For example, following Georgieva et al. (2021) TOI 1260b, $M_{\oplus} = 8.60 + 1.40 - 1.50$, is a super-Earth mass Terrestrial planet that has a rock-ice Terrestrial composition with 50% Earth-

like rocky core and 50% H₂O, or a gas-rich Terrestrial composition with an Earth-like core and approximately 0.1% by mass H-He envelope. The composition modeling for TOI 1260b highlights the usefulness of the composition classification scheme presented in this paper. Based upon the measured radius, TOI 1260b was identified as a “mini-Neptune” by Georgieva et al. (2021). However, the “mini-Neptune” characterization differs significantly from the compositional modeling which indicates the planet has a rock-ice Terrestrial or a gas-rich Terrestrial composition.

Another aspect of the composition classification scheme presented here is that Solar System analog names such as Mercury, Earth, Ganymede, Neptune, Saturn, Jupiter, and “sub” or “super” versions of these names can be consistently applied based upon composition modeling and planetary mass (Table 4). For example, TOI-1260b is a “super-Ganymede” if a rock-ice Terrestrial composition, or a “gas-rich super-Earth” if a gas-rich rock Terrestrial composition (Georgieva et al 2021).

Note that these Solar System analog names make sense when using the planetary mass in combination with the planetary composition models. The resulting characterization will better identify the characteristics of the planet than applying Solar System analog names based upon the planetary radius. The radius of TOI-1260b would classify it as a sub-Neptune, but the planet does not have a Rock-Ice Giant composition as the H-He fraction is much less than 1.0% by mass (Georgieva et al. 2021). With the classification system presented in this paper, Solar System analog names can be consistently used to describe planets based upon their mass and composition derived from M-R-composition models. This approach avoids the inconsistency between name and composition that results when using Solar System analog names based upon the planetary radius alone (e.g. TOI 1260b). As noted in the introduction, Kepler 87c is a super-Earth mass, sub-Saturn radius planet with a Neptune composition (MPB20). Applying the classification scheme presented in this paper, Kepler 87c has a Rock-Ice Giant composition and in combination with its mass can be characterized as a “sub-Neptune”.

Planetary composition models also require knowledge of the stellar flux or equilibrium temperature in order to determine the mass fraction of H-He gas (Lopez & Fortney 2014; Zeng et al. 2019). The planet LTT 3780 c has both mass and radius values nearly identical to those of TOI-1260 b (Table 5). However, the equilibrium temperature of LTT 3780 c is 353 K (Cloutier et al. 2020) whereas the equilibrium temperature of TOI-1260 b is 860 K (Georgieva et al. 2021). As a result of the equilibrium temperature difference, both Lopez & Fortney (2014) and Zeng et al. (2019) models indicate that while TOI-1260 b could have approximately 0.1 percent by mass H-He and is a gas-rich super-Earth, LTT 3780 c has 1-2 percent by mass H-He and is a sub-Neptune. These two planets illustrate the need for equilibrium temperature values in addition to mass and radius data, to improve the determination of the composition class for planets with H-He envelopes.

It is important to note that the composition classification system describes composition characteristics only and not circumstances. For example, the system does not distinguish Rock Terrestrial planets with a solid surface from planets with a molten rock surface, such as lava worlds (Chao et al. 2021). Rock-Ice Terrestrial planets with a supercritical steam envelope are not distinguished from those with an ice surface and sub-surface oceans. These examples illustrate that additional terminology could be added to further describe the physical circumstances of planets.

Finally, the classification scheme can provide a means for consistently characterizing newly discovered exoplanets with names that correctly indicate the planetary composition when communicating those discoveries to students and the general public. For example, many planets characterized as “sub-Neptune” based upon the planetary radius are actually super-Ganymede, gas-rich super-Earth, or gas-rich super-Ganymede planets based upon the mass and composition analysis (e.g. Georgieva et al. 2021; Otegi et al. 2021).

7 Conclusion

This paper was motivated by the need, as discussed in the introduction, for a planetary composition classification system that allows for consistent characterization of currently known and newly discovered exoplanets. Current

characterization of planetary composition in the literature contains significant variation in the usage of terminology and that terminology is sometimes inconsistent with the composition model of the planet.

The composition classification system described in this paper classifies every planet into one of five broad composition classes: Gas Giant, Rock-Ice Giant, gas-rich Terrestrial, Rock Terrestrial, or Rock-Ice Terrestrial. Planets are assigned one of these five composition classes based only upon the mass fractions of H-He gas and rock-ice (Table 1). Each broad composition class is subdivided into multiple possible bulk composition classes using Solar System analog names (Table 4). An important aspect of this classification system is that it covers all currently described composition classes but is flexible to future discoveries as any new or exotic composition classes could be added to the list of bulk composition classes, found in Table 4, without altering the broad and bulk composition classes already described. The composition classification system also does not rely on specific interior structure models and therefore will not require modification as equation of state and interior structure models are revised.

Empirical mass ranges for the composition classes were explored and in combination with the bulk composition classes provide useful guidelines for applying terms such as “super-Earth”, “sub-Neptune”, “super-Ganymede” and other Solar System analog descriptors (Tables 4 & 5).

The familiar terminology utilized for both the broad composition classes and the bulk composition classes, combined with the simplicity and flexibility of the system can facilitate consistent communication of Solar System and exoplanetary discoveries not only in the literature, but also to students and laypersons.

Acknowledgements

This research has made use of the NASA Exoplanet Archive, which is operated by the California Institute of Technology, under contract with the National Aeronautics and Space Administration under the Exoplanet Exploration Program. This research has made use of NASA’s Astrophysics Data System Bibliographic Services. The author would like to thank Ravit Helled and Vardan Adibekyan for helpful comments and suggestions on earlier drafts of this paper.

References

- Adibekyan, V. (2019) Heavy Metal Rules. I. Exoplanet Incidence and Metallicity. *Geosciences* 9, 105. doi:10.3390/geosciences9030105
- Adibekyan V., Dorn C., Sousa S.G., Santos N.C., Bitsch B., Israelian G., Mordasini C., et al. (2021) A compositional link between rocky exoplanets and their host stars. *Science* 374, 330–332. doi:10.1126/science.abg8794
- Aguichine, A., Mousis, O., Deleuil, M., and Marcq, E. (2021) Mass-Radius Relationships for Irradiated Ocean Planets. *The Astrophysical Journal* 914, 84. doi:10.3847/1538-4357/abfa99
- Akeson R.L., Chen X., Ciardi D., Crane M., Good J., Harbut M., and Jackson E., et al. (2013) The NASA Exoplanet Archive: Data and Tools for Exoplanet Research. *Publications of the Astronomical Society of the Pacific* 125, 989. doi:10.1086/672273
- Allen-Sutter, H., Garhart, E., Leinenweber, K., Prakapenka, V., Greenberg, E., and Shim, S.-H. (2020) Oxidation of the Interiors of Carbide Exoplanets. *The Planetary Science Journal* 1, 39. doi:10.3847/PSJ/abaa3e
- Armstrong D.J., Lopez T.A., Adibekyan V., Booth R.A., Bryant E.M., Collins K.A., and Deleuil M., et al. (2020) A remnant planetary core in the hot-Neptune desert. *Nature* 583, 39–42. doi:10.1038/s41586-020-2421-7

- Azevedo Silva T., Demangeon O.D.S., Barros S.C.C., Armstrong D.J., Otegi J.F., Bossini D., Delgado Mena E., et al. (2022) The HD 137496 system: A dense, hot super-Mercury and a cold Jupiter. *Astronomy and Astrophysics* 657, A68. doi:10.1051/0004-6361/202141520
- Baraffe, I., Chabrier, G., and Barman, T. (2008) Structure and evolution of super-Earth to super-Jupiter exoplanets. I. Heavy element enrichment in the interior. *Astronomy and Astrophysics* 482, 315–332. doi:10.1051/0004-6361:20079321
- Baraffe, I., Chabrier, G., and Barman, T. (2010) The physical properties of extra-solar planets. *Reports on Progress in Physics* 73. doi:10.1088/0034-4885/73/1/016901
- Baraffe, I., Chabrier, G., Fortney, J., and Sotin, C. (2014) Planetary Internal Structures. *Protostars and Planets VI*, 763-786. Henrik Beuther, Ralf S. Klessen, Cornelis P. Dullemond, and Thomas Henning (eds.), University of Arizona Press, Tucson. doi:10.2458/azu_uapress_9780816531240-ch033
- Bashi, D., Helled, R., Zucker, S., and Mordasini, C. (2017) Two empirical regimes of the planetary mass-radius relation. *Astronomy and Astrophysics* 604, 83. doi:10.1051/0004-6361/201629922
- Bean, J.L., Raymond, S.N., and Owen, J.E. (2021) The Nature and Origins of Sub-Neptune Size Planets. *Journal of Geophysical Research (Planets)* 126. doi:10.1029/2020JE006639
- Bedell M., Bean J.L., Meléndez J., Spina L., Ramírez I., Asplund M., and Alves-Brito A., et al. (2018) The Chemical Homogeneity of Sun-like Stars in the Solar Neighborhood. *The Astrophysical Journal* 865, 68. doi:10.3847/1538-4357/aad908
- Bitsch, B. and Battistini, C. (2020) Influence of sub- and super-solar metallicities on the composition of solid planetary building blocks. *Astronomy and Astrophysics* 633, 10. doi:10.1051/0004-6361/201936463
- Bodenheimer, P., D'Angelo, G., Lissauer, J.J., Fortney, J.J., and Saumon, D. (2013) Deuterium Burning in Massive Giant Planets and Low-mass Brown Dwarfs Formed by Core-nucleated Accretion. *The Astrophysical Journal* 770, 120. doi:10.1088/0004-637X/770/2/120
- Bond, J.C., O'Brien, D.P., and Lauretta, D.S. (2010) The Compositional Diversity of Extrasolar Terrestrial Planets. I. In Situ Simulations. *The Astrophysical Journal* 715, 1050–1070. doi:10.1088/0004-637X/715/2/1050
- Bonomo A.S., Hébrard G., Raymond S.N., Bouchy F., Lecavelier des Etangs A., Bordé P., Aigrain S., et al., (2017) A deeper view of the CoRoT-9 planetary system. A small non-zero eccentricity for CoRoT-9b likely generated by planet-planet scattering. *Astronomy and Astrophysics* 603, A43. doi:10.1051/0004-6361/201730624
- Bonomo A.S., Zeng L., Damasso M., Leinhardt Z.M., Justesen A.B., Lopez E., Lund M.N., et al. (2019) A giant impact as the likely origin of different twins in the Kepler-107 exoplanet system. *Nature Astronomy* 3, 416–423. doi:10.1038/s41550-018-0684-9
- Boss, A.P. (2001) Gas Giant Protoplanet Formation: Disk Instability Models with Thermodynamics and Radiative Transfer. *The Astrophysical Journal* 563, 367–373. doi:10.1086/323694
- Boss, A.P. (2003) Rapid Formation of Outer Giant Planets by Disk Instability. *The Astrophysical Journal* 599, 577–581. doi:10.1086/379163
- Caballero, J.A. (2018) A Review on Substellar Objects below the Deuterium Burning Mass Limit: Planets, Brown Dwarfs or What?. *Geosciences* 8, 362. doi:10.3390/geosciences8100362
- Cañas C.I., Stefansson G., Kanodia S., Mahadevan S., Cochran W.D., Endl M., Robertson P., et al. (2020) A Warm Jupiter Transiting an M Dwarf: A TESS Single-transit Event Confirmed with the Habitable-zone Planet Finder. *The Astronomical Journal* 160, 147. doi:10.3847/1538-3881/abac67

- Carleo I., Gandolfi D., Barragán O., Livingston J.H., Persson C.M., Lam K.W.F., Vidotto A., et al. (2020) The Multiplanet System TOI-421. *The Astronomical Journal* 160, 114. doi:10.3847/1538-3881/aba124
- Chabrier, G., Johansen, A., Janson, M., and Rafikov, R. (2014) Giant Planet and Brown Dwarf Formation. *Protostars and Planets VI*, 619. doi:10.2458/azu_uapress_9780816531240-ch027
- Chachan Y., Dalba P.A., Knutson H.A., Fulton B.J., Thorngren D., Beichman C., Ciardi D.R., et al. (2022) Kepler-167e as a Probe of the Formation Histories of Cold Giants with Inner Super-Earths. *The Astrophysical Journal* 926, 62. doi:10.3847/1538-4357/ac3ed6
- Chao, K.-H., deGraffenried, R., Lach, M., Nelson, W., Truax, K., and Gaidos, E. (2021) Lava worlds: From early earth to exoplanets. *Chemie der Erde / Geochemistry* 81, 125735. doi:10.1016/j.chemer.2020.125735
- Chen, J. and Kipping, D. (2017) Probabilistic Forecasting of the Masses and Radii of Other Worlds. *The Astrophysical Journal* 834, 17. doi:10.3847/1538-4357/834/1/17
- Cloutier R., Eastman J.D., Rodriguez J.E., Astudillo-Defru N., Bonfils X., Mortier A., Watson C.A., et al. (2020) A Pair of TESS Planets Spanning the Radius Valley around the Nearby Mid-M Dwarf LTT 3780. *The Astronomical Journal* 160, 3. doi:10.3847/1538-3881/ab91c2
- Cloutier R., Charbonneau D., Deming D., Bonfils X., Astudillo-Defru N., (2021) A More Precise Mass for GJ 1214 b and the Frequency of Multiplanet Systems Around Mid-M Dwarfs. *The Astronomical Journal* 162, 174. doi:10.3847/1538-3881/ac1584
- Dai, F., Masuda, K., Winn, J.N., and Zeng, L. (2019) Homogeneous Analysis of Hot Earths: Masses, Sizes, and Compositions. *The Astrophysical Journal* 883, 79. doi:10.3847/1538-4357/ab3a3b
- Dalba P.A., Kane S.R., Li Z., MacDougall M.G., Rosenthal L.J., Cherubim C., Isaacson H., et al. (2021) Giant Outer Transiting Exoplanet Mass (GOT 'EM) Survey. II. Discovery of a Failed Hot Jupiter on a 2.7 Yr, Highly Eccentric Orbit. *The Astronomical Journal* 162, 154. doi:10.3847/1538-3881/ac134b
- Delrez L., Ehrenreich D., Alibert Y., Bonfanti A., Borsato L., Fossati L., Hooton M.J., et al. (2021) Transit detection of the long-period volatile-rich super-Earth V² Lupi d with CHEOPS. *Nature Astronomy* 5, 775–787. doi:10.1038/s41550-021-01381-5
- Demangeon O.D.S., Zapatero Osorio M.R., Alibert Y., Barros S.C.C., Adibekyan V., Tabernero H.M., Antoniadis-Karnavas A., et al. (2021) Warm terrestrial planet with half the mass of Venus transiting a nearby star. *Astronomy and Astrophysics* 653, A41. doi:10.1051/0004-6361/202140728
- de Pater, I. and Lissauer, J.J. (2015) *Planetary Sciences*. Planetary Sciences, by Imke de Pater, Jack J. Lissauer, Cambridge, UK: Cambridge University Press, 2015.
- Dorn C., Khan A., Heng K., Connolly J.A.D., Alibert Y., Benz W., and Tackley P. (2015) Can we constrain the interior structure of rocky exoplanets from mass and radius measurements?. *Astronomy and Astrophysics* 577, 83. doi:10.1051/0004-6361/201424915
- Dorn C., Venturini J., Khan A., Heng K., Alibert Y., Helled R., and Rivoldini A., et al. (2017) A generalized Bayesian inference method for constraining the interiors of super Earths and sub-Neptunes. *Astronomy and Astrophysics* 597, 37. doi:10.1051/0004-6361/201628708
- Dragomir D., Teske J., Günther M.N., Ségransan D., Burt J.A., Huang C.X., Vanderburg A., et al. (2019) TESS Delivers Its First Earth-sized Planet and a Warm Sub-Neptune. *The Astrophysical Journal* 875, L7. doi:10.3847/2041-8213/ab12ed

- Ellis T.G., Boyajian T., von Braun K., Ligi R., Mourard D., Dragomir D., Schaefer G.H., et al. (2021) Directly Determined Properties of HD 97658 from Interferometric Observations. *The Astronomical Journal* 162, 118. doi:10.3847/1538-3881/ac141a
- Espinoza N., Brahm R., Henning T., Jordán A., Dorn C., Rojas F., Sarkis P., et al. (2020) HD 213885b: a transiting 1-d-period super-Earth with an Earth-like composition around a bright ($V = 7.9$) star unveiled by TESS. *Monthly Notices of the Royal Astronomical Society* 491, 2982–2999. doi:10.1093/mnras/stz3150
- Fortney, J.J., Marley, M.S., and Barnes, J.W. (2007) Planetary Radii across Five Orders of Magnitude in Mass and Stellar Insolation: Application to Transits. *The Astrophysical Journal* 659, 1661–1672. doi:10.1086/512120
- Fortney, J.J. (2012) On the Carbon-to-oxygen Ratio Measurement in nearby Sun-like Stars: Implications for Planet Formation and the Determination of Stellar Abundances. *The Astrophysical Journal* 747, 27. doi:10.1088/2041-8205/747/2/L27
- Fridlund M., Livingston J., Gandolfi D., Persson C.M., Lam K.W.F., Stassun K.G., Hellier C., et al. (2020) The TOI-763 system: sub-Neptunes orbiting a Sun-like star. *Monthly Notices of the Royal Astronomical Society* 498, 4503. doi:10.1093/mnras/staa2502
- Fulton B.J., Petigura E.A., Howard A.W., Isaacson H., Marcy G.W., Cargile P.A., and Hebb L., et al. (2017) The California-Kepler Survey. III. A Gap in the Radius Distribution of Small Planets. *The Astronomical Journal* 154, 109. doi:10.3847/1538-3881/aa80eb
- Georgieva I.Y., Persson C.M., Barragán O., Nowak G., Fridlund M., Locci D., and Palte E., et al. (2021) Hot planets around cool stars - two short-period mini-Neptunes transiting the late K-dwarf TOI-1260. *Monthly Notices of the Royal Astronomical Society* 505, 4684–4701. doi:10.1093/mnras/stab1464
- Gettel S., Charbonneau D., Dressing C.D., Buchhave L.A., Dumusque X., Vanderburg A., Bonomo A.S., et al. (2016) The Kepler-454 System: A Small, Not-rocky Inner Planet, a Jovian World, and a Distant Companion. *The Astrophysical Journal* 816, 95. doi:10.3847/0004-637X/816/2/95
- Gill S., Wheatley P.J., Cooke B.F., Jordán A., Nielsen L.D., Bayliss D., Anderson D.R., et al. (2020) NGTS-11 b (TOI-1847 b): A Transiting Warm Saturn Recovered from a TESS Single-transit Event. *The Astrophysical Journal* 898, L11. doi:10.3847/2041-8213/ab9eb9
- Goda, S. and Matsuo, T. (2019) Multiple Populations of Extrasolar Gas Giants. *The Astrophysical Journal* 876, 23. doi:10.3847/1538-4357/ab0f9c
- Grasset, O., Schneider, J., and Sotin, C. (2009) A Study of the Accuracy of Mass-Radius Relationships for Silicate-Rich and Ice-Rich Planets up to 100 Earth Masses. *The Astrophysical Journal* 693, 722–733. doi:10.1088/0004-637X/693/1/722
- Gupta, A. and Schlichting, H.E. (2021) Caught in the act: core-powered mass-loss predictions for observing atmospheric escape. *Monthly Notices of the Royal Astronomical Society* 504, 4634–4648. doi:10.1093/mnras/stab1128
- Hadden S. and Lithwick Y. (2017) Kepler Planet Masses and Eccentricities from TTV Analysis. *The Astronomical Journal* 154, 5. doi:10.3847/1538-3881/aa71ef
- Hakim K., Rivoldini A., Van Hoolst T., Cottenier S., Jaeken J., Chust T., and Steinle-Neumann G. (2018a) A new ab initio equation of state of hcp-Fe and its implication on the interior structure and mass-radius relations of rocky super-Earths. *Icarus* 313, 61–78. doi:10.1016/j.icarus.2018.05.005
- Hakim, K., van Westrenen, W., and Dominik, C. (2018b) Capturing the oxidation of silicon carbide in rocky exoplanetary interiors. *Astronomy and Astrophysics* 618, 6. doi:10.1051/0004-6361/201833942

- Hakim K., Spaargaren R., Grewal D.S., Rohrbach A., Berndt J., Dominik C., and van Westrenen W. (2019a) Mineralogy, Structure, and Habitability of Carbon-Enriched Rocky Exoplanets: A Laboratory Approach. *Astrobiology* 19, 867–884. doi:10.1089/ast.2018.1930
- Hakim, K., van den Berg, A., Vazan, A., Höning, D., van Westrenen, W., and Dominik, C. (2019b) Thermal evolution of rocky exoplanets with a graphite outer shell. *Astronomy and Astrophysics* 630, 152. doi:10.1051/0004-6361/201935714
- Hamann A., Montet B.T., Fabrycky D.C., Agol E., and Kruse E. (2019) K2-146: Discovery of Planet c, Precise Masses from Transit Timing, and Observed Precession. *The Astronomical Journal*, 158, 133. doi:10.3847/1538-3881/ab32e3
- Hatzes, A.P. and Rauer, H. (2015) A Definition for Giant Planets Based on the Mass-Density Relationship. *The Astrophysical Journal* 810, L25. doi:10.1088/2041-8205/810/2/L25
- Hébrard G., Bonomo A.S., Díaz R.F., Santerne A., Santos N.C., Almenara J.-M., Barros S.C.C., et al. (2019) SOPHIE velocimetry of Kepler transit candidates. XIX. The transiting temperate giant planet KOI-3680b. *Astronomy and Astrophysics* 623, A104. doi:10.1051/0004-6361/201834333
- Helled, R. and Stevenson, D. (2017) The Fuzziness of Giant Planets' Cores. *The Astrophysical Journal* 840, L4. doi:10.3847/2041-8213/aa6d08
- Helled, R. (2018) The Interiors of Jupiter and Saturn. *Oxford Research Encyclopedia of Planetary Science*. doi:10.1093/acrefore/9780190647926.013.175
- Helled, R., Nettelmann, N., and Guillot, T. (2020) Uranus and Neptune: Origin, Evolution and Internal Structure. *Space Science Reviews* 216, 38. doi:10.1007/s11214-020-00660-3
- Helled, R. and Fortney, J.J. (2020) The interiors of Uranus and Neptune: current understanding and open questions. *Philosophical Transactions of the Royal Society of London Series A* 378. doi:10.1098/rsta.2019.0474
- Hirano T., Livingston J.-H., Fukui A., Narita N., Harakawa H., Ishikawa H.-T., Miyakawa K., et al. (2021) Two Bright M Dwarfs Hosting Ultra-Short-Period Super-Earths with Earth-like Compositions. *The Astronomical Journal* 162, 161. doi:10.3847/1538-3881/ac0fdc
- Huang C.X., Burt J., Vanderburg A., Günther M.N., Shporer A., Dittmann J.A., Winn J.N., et al. (2018) TESS Discovery of a Transiting Super-Earth in the π Mensae System. *The Astrophysical Journal*, 868, L39. doi:10.3847/2041-8213/aaef91
- Huang C., Rice D.R., Grande Z.M., Smith D., Smith J.S., Boisvert J.H., and Tschauer O., et al. (2021) Implications of an improved water equation of state for water-rich planets. *Monthly Notices of the Royal Astronomical Society* 503, 2825–2832. doi:10.1093/mnras/stab645
- Jontof-Hutter D., Ford E.B., Rowe J.F., Lissauer J.J., Fabrycky D.C., Van Laerhoven C., Agol E., et al. (2016) Secure Mass Measurements from Transit Timing: 10 Kepler Exoplanets between 3 and 8 M_{\oplus} . *The Astrophysical Journal* 820, 39. doi:10.3847/0004-637X/820/1/39
- Jontof-Hutter, D. (2019) The Compositional Diversity of Low-Mass Exoplanets. *Annual Review of Earth and Planetary Sciences* 47, 141–171. doi:10.1146/annurev-earth-053018-060352
- Kipping, D. (2021) The exomoon corridor: Half of all exomoons exhibit TTV frequencies within a narrow window due to aliasing. *Monthly Notices of the Royal Astronomical Society* 500, 1851–1857. doi:10.1093/mnras/staa3398
- Kossakowski D., Kemmer J., Bluhm P., Stock S., Caballero J.A., Béjar V.J.S., Cardona Guillén C., et al. (2021) TOI-1201 b: A mini-Neptune transiting a bright and moderately young M dwarf. *arXiv: arXiv:2109.09346*
- Kumar, S.S. (1963) The Structure of Stars of Very Low Mass. *The Astrophysical Journal* 137, 1121. doi:10.1086/147589

- Lacedelli G., Malavolta L., Borsato L., Piotto G., Nardiello D., Mortier A., and Stalport M., et al. (2021) An unusually low density ultra-short period super-Earth and three mini-Neptunes around the old star TOI-561. *Monthly Notices of the Royal Astronomical Society* 501, 4148–4166. doi:10.1093/mnras/staa3728
- Lambrechts M., Johansen A., and Morbidelli A. (2014) Separating gas-giant and ice-giant planets by halting pebble accretion. *Astronomy and Astrophysics* 572, A35. doi:10.1051/0004-6361/201423814
- Leleu A., Alibert Y., Hara N.C., Hooton M.J., Wilson T.G., Robutel P., Delisle J.-B., et al. (2021) Six transiting planets and a chain of Laplace resonances in TOI-178. *Astronomy and Astrophysics* 649, A26. doi:10.1051/0004-6361/202039767
- Lecavelier des Etangs A. and Lissauer J.J. (2022) The IAU working definition of an exoplanet. *New Astronomy Reviews* 94, 101641. doi:10.1016/j.newar.2022.101641
- Libby-Roberts J.E., Berta-Thompson Z.K., Désert J.-M., Masuda K., Morley C.-V., Lopez E.-D., Deck K.-M., et al. (2020) The Featureless Transmission Spectra of Two Super-puff Planets. *The Astronomical Journal* 159, 57. doi:10.3847/1538-3881/ab5d36
- Lillo-Box J., Figueira P., Leleu A., Acuña L., Faria J.P., Hara N., Santos N.C., et al. (2020a) Planetary system LHS 1140 revisited with ESPRESSO and TESS. *Astronomy and Astrophysics* 642, A121. doi:10.1051/0004-6361/202038922
- Lillo-Box J., Lopez T.A., Santerne A., Nielsen L.D., Barros S.C.C., Deleuil M., Acuña L., et al. (2020b) Masses for the seven planets in K2-32 and K2-233. Four diverse planets in resonant chain and the first young rocky worlds. *Astronomy and Astrophysics* 640, A48. doi:10.1051/0004-6361/202037896
- Lineweaver, C.H. and Norman, M. (2010) The Potato Radius: a Lower Minimum Size for Dwarf Planets. arXiv e-prints. arXiv:1004.1091
- Lingam M. and Loeb A. (2019) Dependence of Biological Activity on the Surface Water Fraction of Planets. *The Astronomical Journal*, 157, 25. doi:10.3847/1538-3881/aaf420
- Lopez, E.D. and Fortney, J.J. (2014) Understanding the Mass-Radius Relation for Sub-neptunes: Radius as a Proxy for Composition. *The Astrophysical Journal* 792, 1. doi:10.1088/0004-637X/792/1/1
- Lopez T.A., Barros S.C.C., Santerne A., Deleuil M., Adibekyan V., Almenara J.-M., Armstrong D.J., et al. (2019) Exoplanet characterisation in the longest known resonant chain: the K2-138 system seen by HARPS. *Astronomy and Astrophysics* 631, A90. doi:10.1051/0004-6361/201936267
- López-Morales M., Haywood R.D., Coughlin J.L., Zeng L., Buchhave L.A., Giles H.A.C., and Affer L., et al. (2016) Kepler-21b: A Rocky Planet Around a $V = 8.25$ Magnitude Star. *The Astronomical Journal* 152, 204. doi:10.3847/0004-6256/152/6/204
- Lozovsky, M., Helled, R., Dorn, C., and Venturini, J. (2018) Threshold Radii of Volatile-rich Planets. *The Astrophysical Journal* 866, 49. doi:10.3847/1538-4357/aadd09
- Lubin J., Van Zandt J., Holcomb R., Weiss L.M., Petigura E.A., Robertson P., Akana Murphy J.M., et al. (2022) TESS-Keck Survey. IX. Masses of Three Sub-Neptunes Orbiting HD 191939 and the Discovery of a Warm Jovian plus a Distant Substellar Companion. *The Astronomical Journal* 163, 101. doi:10.3847/1538-3881/ac3d38
- Luhman, K.L. and Hapich, C.J. (2020) New Candidates for Planetary-mass Brown Dwarfs in IC 348. *The Astronomical Journal* 160, 57. doi:10.3847/1538-3881/ab96bb
- Luque R., Nowak G., Pallé E., Dai F., Kaminski A., Nagel E., Hidalgo D., et al. (2019) Detection and characterization of an ultra-dense sub-Neptunian planet orbiting the Sun-like star K2-292. *Astronomy and Astrophysics* 623, A114. doi:10.1051/0004-6361/201834952

- Luque R., Serrano L.M., Molaverdikhani K., Nixon M.C., Livingston J.H., Guenther E.W., Pallé E., et al. (2021) A planetary system with two transiting mini-Neptunes near the radius valley transition around the bright M dwarf TOI-776. *Astronomy and Astrophysics* 645 A41. doi:10.1051/0004-6361/202039455
- Ma, B. and Ge, J. (2014) Statistical properties of brown dwarf companions: implications for different formation mechanisms. *Monthly Notices of the Royal Astronomical Society* 439, 2781–2789. doi:10.1093/mnras/stu134
- MacDonald M.G., Ragozzine D., Fabrycky D.C., Ford E.B., Holman M.J., Isaacson H.T., Lissauer J.J., et al. (2016) A Dynamical Analysis of the Kepler-80 System of Five Transiting Planets. *The Astronomical Journal* 152, 105. doi:10.3847/0004-6256/152/4/105
- MacDougall M.G., Petigura E.A., Angelo I., Lubin J., Batalha N.M., Beard C., Behrard A., et al. (2021) The TESS-Keck Survey. VI. Two Eccentric sub-Neptunes Orbiting HIP-97166. arXiv, arXiv:2110.05628
- Mancini L., Lillo-Box J., Southworth J., Borsato L., Gandolfi D., Ciceri S., Barrado D., et al. (2016) Kepler-539: A young extrasolar system with two giant planets on wide orbits and in gravitational interaction. *Astronomy and Astrophysics* 590, A112. doi:10.1051/0004-6361/201526357
- Marcy G.W., Isaacson H., Howard A.W., Rowe J.F., Jenkins J.M., Bryson S.T., Latham D.W., et al. (2014) Masses, Radii, and Orbits of Small Kepler Planets: The Transition from Gaseous to Rocky Planets. *The Astrophysical Journal Supplement* 210, 20. doi:10.1088/0067-0049/210/2/20
- Mayo A.W., Rajpaul V.M., Buchhave L.A., Dressing C.D., Mortier A., Zeng L., Fortenbach C.D., et al. (2019) An 11 Earth-mass, Long-period Sub-Neptune Orbiting a Sun-like Star. *The Astronomical Journal* 158, 165. doi:10.3847/1538-3881/ab3e2f
- Mazevet, S., Licari, A., Chabrier, G., and Potekhin, A.Y. (2019) Ab initio based equation of state of dense water for planetary and exoplanetary modeling. *Astronomy and Astrophysics* 621, 128. doi:10.1051/0004-6361/201833963
- Mercer, A. and Stamatellos, D. (2020) Planet formation around M dwarfs via disc instability. Fragmentation conditions and protoplanet properties. *Astronomy and Astrophysics* 633, 116. doi:10.1051/0004-6361/201936954
- Miller N., Fortney J.J. (2011) The Heavy-element Masses of Extrasolar Giant Planets, Revealed. *The Astrophysical Journal* 736, L29. doi:10.1088/2041-8205/736/2/L29
- Millholland, S., Petigura, E., and Batygin, K. (2020) Tidal Inflation Reconciles Low-density Sub-Saturns with Core Accretion. *The Astrophysical Journal* 897, 7. doi:10.3847/1538-4357/ab959c (MPB20)
- Mills S.M., Fabrycky D.C., Migaszewski C., Ford E.B., Petigura E., and Isaacson H. (2016) A resonant chain of four transiting, sub-Neptune planets. *Nature* 533, 509–512. doi:10.1038/nature17445
- Miozzi F., Morard G., Antonangeli D., Clark A.N., Mezouar M., Dorn C., and Rozel A., et al. (2018) Equation of State of SiC at Extreme Conditions: New Insight Into the Interior of Carbon-Rich Exoplanets. *Journal of Geophysical Research (Planets)* 123, 2295–2309. doi:10.1029/2018JE005582
- Misener, W. and Schlichting, H.E. (2021) To cool is to keep: residual H/He atmospheres of super-Earths and sub-Neptunes. *Monthly Notices of the Royal Astronomical Society* 503, 5658–5674. doi:10.1093/mnras/stab895
- Morbidelli, A., Lambrechts, M., Jacobson, S., and Bitsch, B. (2015) The great dichotomy of the Solar System: Small terrestrial embryos and massive giant planet cores. *Icarus* 258, 418–429. doi:10.1016/j.icarus.2015.06.003
- Mortier A., Bonomo A.S., Rajpaul V.M., Buchhave L.A., Vanderburg A., Zeng L., López-Morales M., et al. (2018) K2-263 b: a 50 d period sub-Neptune with a mass measurement using HARPS-N. *Monthly Notices of the Royal Astronomical Society* 481, 1839. doi:10.1093/mnras/sty2360

- Mortier A., Zapatero Osorio M.R., Malavolta L., Alibert Y., Rice K., Lillo-Box J., Vanderburg A., et al. (2020) K2-111: an old system with two planets in near-resonance. *Monthly Notices of the Royal Astronomical Society* 499, 5004. doi:10.1093/mnras/staa3144
- Mousis O., Deleuil M., Aguichine A., Marcq E., Naar J., Aguirre L.A., and Brugger B., et al. (2020) Irradiated Ocean Planets Bridge Super-Earth and Sub-Neptune Populations. *The Astrophysical Journal* 896, 22. doi:10.3847/2041-8213/ab9530
- Narang M., Manoj P., Furlan E., Mordasini C., Henning T., Mathew B., and R.K., et al. (2018) Properties and Occurrence Rates for Kepler Exoplanet Candidates as a Function of Host Star Metallicity from the DR25 Catalog. *The Astronomical Journal* 156, 221. doi:10.3847/1538-3881/aae391
- Nielsen L.D., Gandolfi D., Armstrong D.J., Jenkins J.S., Fridlund M., Santos N.C., and Dai F. et al. (2020) Mass determinations of the three mini-Neptunes transiting TOI-125. *Monthly Notices of the Royal Astronomical Society* 492, 5399–5412. doi:10.1093/mnras/staa197
- Nowak G., Luque R., Parviainen H., Pallé E., Molaverdikhani K., Béjar V.J.S., Lillo-Box J., et al. (2020) The CARMENES search for exoplanets around M dwarfs. Two planets on opposite sides of the radius gap transiting the nearby M dwarf LTT 3780. *Astronomy and Astrophysics* 642, A173. doi:10.1051/0004-6361/202037867
- Ogihara, M., Hori, Y., Kunitomo, M., and Kurosaki, K. (2021) Formation of giant planets with large metal masses and metal fractions via giant impacts in a rapidly dissipating disk. *Astronomy and Astrophysics* 648, 1. doi:10.1051/0004-6361/202140464
- Osborn H.P., Armstrong D.J., Adibekyan V., Collins K.A., Delgado-Mena E., Howell S.B., and Hellier C., et al. (2021) A hot mini-Neptune in the radius valley orbiting solar analogue HD 110113. *Monthly Notices of the Royal Astronomical Society* 502, 4842–4857. doi:10.1093/mnras/stab182
- Otegi, J.F., Bouchy, F., and Helled, R. (2020) Revisited mass-radius relations for exoplanets below $120 M_{\oplus}$. *Astronomy and Astrophysics* 634. doi:10.1051/0004-6361/201936482 (OBH20)
- Otegi J.F., Bouchy F., Helled R., Armstrong D.J., Stalport M., Stassun K.G., and Delgado-Mena E., et al. (2021) TESS and HARPS reveal two sub-Neptunes around TOI 1062. *Astronomy and Astrophysics* 653. doi:10.1051/0004-6361/202040247
- Owen, J.E. and Mohanty, S. (2016) Habitability of terrestrial-mass planets in the HZ of M Dwarfs - I. H/He-dominated atmospheres. *Monthly Notices of the Royal Astronomical Society* 459, 4088–4108. doi:10.1093/mnras/stw959
- Owen, J.E., Shaikhislamov, I.F., Lammer, H., Fossati, L., and Khodachenko, M.L. (2020) Hydrogen Dominated Atmospheres on Terrestrial Mass Planets: Evidence, Origin and Evolution. *Space Science Reviews* 216, 129. doi:10.1007/s11214-020-00756-w
- Palle E., Nowak G., Luque R., Hidalgo D., Barragán O., Prieto-Arranz J., Hirano T., et al. (2019) Detection and Doppler monitoring of K2-285 (EPIC 246471491), a system of four transiting planets smaller than Neptune. *Astronomy and Astrophysics* 623, A41. doi:10.1051/0004-6361/201834001
- Petigura E.A., Sinukoff E., Lopez E.D., Crossfield I.J.M., Howard A.W., Brewer J.M., and Fulton B.J., et al. (2017) Four Sub-Saturns with Dissimilar Densities: Windows into Planetary Cores and Envelopes. *The Astronomical Journal* 153, 142. doi:10.3847/1538-3881/aa5ea5
- Petigura E.A., Livingston J., Batygin K., Mills S.M., Werner M., Isaacson H., Fulton B.J., et al. (2020) K2-19b and c are in a 3:2 Commensurability but out of Resonance: A Challenge to Planet Assembly by Convergent Migration. *The Astronomical Journal* 159, 2. doi:10.3847/1538-3881/ab5220

- Raetz, S., Heras, A.M., Fernández, M., Casanova, V., and Marka, C. (2019) Transit analysis of the CoRoT-5, CoRoT-8, CoRoT-12, CoRoT-18, CoRoT-20, and CoRoT-27 systems with combined ground- and space-based photometry. *Monthly Notices of the Royal Astronomical Society* 483, 824–839. doi:10.1093/mnras/sty3085
- Raymond S.N., Izidoro A., and Morbidelli A. (2018) arXiv e-prints, arXiv:1812.01033
- Rice K., Malavolta L., Mayo A., Mortier A., Buchhave L.A., Affer L., Vanderburg A., et al. (2019) Masses and radii for the three super-Earths orbiting GJ 9827, and implications for the composition of small exoplanets. *Monthly Notices of the Royal Astronomical Society* 484, 3731. doi:10.1093/mnras/stz130
- Russell, D.G. (2017) The Moon Meets All Requirements of the IAU Definition for “Planet”. *International Journal of Astronomy and Astrophysics* 7, 291–302. doi:10.4236/ijaa.2017.74024
- Santos N.C., Adibekyan V., Dorn C., Mordasini C., Noack L., Barros S.C.C., and Delgado-Mena E., et al. (2017) Constraining planet structure and composition from stellar chemistry: trends in different stellar populations. *Astronomy and Astrophysics* 608, 94. doi:10.1051/0004-6361/201731359
- Schlaufman, K.C. (2018) Evidence of an Upper Bound on the Masses of Planets and Its Implications for Giant Planet Formation. *The Astrophysical Journal* 853, 37. doi:10.3847/1538-4357/aa961c
- Schubert G., Hussmann H., Lainey V., Matson D.L., McKinnon W.B., Sohl F., and Sotin C., et al. (2010) Evolution of Icy Satellites. *Space Science Reviews* 153, 447–484. doi:10.1007/s11214-010-9635-1
- Seidel J.V., Lendl M., Bourrier V., Ehrenreich D., Allart R., Sousa S.G., Cegla H.M., et al. (2020) Hot Exoplanet Atmospheres Resolved with Transit Spectroscopy (HEARTS). VI. Non-detection of sodium with HARPS on the bloated super-Neptune WASP-127b. *Astronomy and Astrophysics* 643, A45. doi:10.1051/0004-6361/202039058
- Sotin, C., Jackson, J.M., and Seager, S. (2010) *Terrestrial Planet Interiors*. Exoplanets 375–395, edited by S. Seager. Tucson, AZ: University of Arizona Press.
- Sozzetti A., Damasso M., Bonomo A.~S., Alibert Y., Sousa S.G., Adibekyan V., Zapatero Osorio M.R., et al. (2021) A sub-Neptune and a non-transiting Neptune-mass companion unveiled by ESPRESSO around the bright late-F dwarf HD 5278 (TOI-130). *Astronomy and Astrophysics* 648, A75. doi:10.1051/0004-6361/202040034
- Stern, S.A. and Levison, H.F. (2002) Regarding the criteria for planethood and proposed planetary classification schemes. *Highlights of Astronomy* 12, 205–213.
- Stern, S.A., Gladstone, R., Zangari, A., Fleming, T., and Goldstein, D. (2015) Transient atmospheres on Charon and water-ice covered KBOs resulting from comet impacts. *Icarus* 246, 298–302. doi:10.1016/j.icarus.2014.03.008
- Suárez-Andrés L., Israelian G., González Hernández J.I., Adibekyan V.Z., Delgado Mena E., Santos N.C., and Sousa S.G. (2017) C/O vs Mg/Si ratios in solar-type stars: The HARPS sample. *Highlights on Spanish Astrophysics IX*, 567–572.
- Sun L., Ioannidis P., Gu S., Schmitt J.H.M.M., Wang X., Kouwenhoven M.B.N. (2019) Kepler-411: a four-planet system with an active host star. *Astronomy and Astrophysics* 624, A15. doi:10.1051/0004-6361/201834275
- Tancredi, G. (2010) Physical and dynamical characteristics of icy dwarf planets (plutoids). *Icy Bodies of the Solar System* 263, 173–185. doi:10.1017/S1743921310001717
- Teanby, N.A., Irwin, P.G.J., Moses, J.I., and Helled, R. (2020) Neptune and Uranus: ice or rock giants?. *Philosophical Transactions of the Royal Society of London Series A* 378. doi:10.1098/rsta.2019.0489
- Trifonov T., Caballero J.A., Morales J.C., Seifahrt A., Ribas I., Reiners A., Bean J.L., et al. (2021) A nearby transiting rocky exoplanet that is suitable for atmospheric investigation. *Science* 371, 1038–1041. doi:10.1126/science.abd7645

- Turbet M., Bolmont E., Ehrenreich D., Gratier P., Leconte J., Selsis F., and Hara N., et al. (2020) Revised mass-radius relationships for water-rich rocky planets more irradiated than the runaway greenhouse limit. *Astronomy and Astrophysics* 638, 41. doi:10.1051/0004-6361/201937151
- Turner J.D., Pearson K.A., Biddle L.I., Smart B.M., Zellem R.T., Teske J.K., Hardegree-Ullman K.K., et al. (2016) Ground-based near-UV observations of 15 transiting exoplanets: constraints on their atmospheres and no evidence for asymmetrical transits. *Monthly Notices of the Royal Astronomical Society* 459, 789–819. doi:10.1093/mnras/stw574
- Untertorn, C.T., Hull, S.D., Stixrude, L., Teske, J.K., Johnson, J.A., and Panero, W.R. (2017) Stellar Chemical Clues as to the Rarity of Exoplanetary Tectonics. *Habitable Worlds 2017: A System Science Workshop* 2042.
- Vance S.D., Panning M.P., Stähler S., Cammarano F., Bills B.G., Tobie G., Kamata S., et al. (2018) Geophysical Investigations of Habitability in Ice-Covered Ocean Worlds. *Journal of Geophysical Research (Planets)*, 123, 180. doi:10.1002/2017JE005341
- Vanderburg A., Becker J.C., Buchhave L.A., Mortier A., Lopez E., Malavolta L., and Haywood R.D., et al. (2017) Precise Masses in the WASP-47 System. *The Astronomical Journal* 154, 237. doi:10.3847/1538-3881/aa918b
- Van Eylen V., Astudillo-Defru N., Bonfils X., Livingston J., Hirano T., Luque R., Lam K.W.F., et al. (2021) Masses and compositions of three small planets orbiting the nearby M dwarf L231-32 (TOI-270) and the M dwarf radius valley. *Monthly Notices of the Royal Astronomical Society*, 507, 2154. doi:10.1093/mnras/stab2143
- Vazan, A., Sari, R., and Kessel, R. (2022) A New Perspective on the Interiors of Ice-rich Planets: Ice-Rock Mixture Instead of Ice on Top of Rock. *The Astrophysical Journal* 926. doi:10.3847/1538-4357/ac458c
- Vissapragada S., Jontof-Hutter D., Shporer A., Knutson H.~A., Liu L., Thorngren D., Lee E.~J., et al. (2020) Diffuser-assisted Infrared Transit Photometry for Four Dynamically Interacting Kepler Systems. *The Astronomical Journal* 159, 108. doi:10.3847/1538-3881/ab65c8
- Wahl S.M., Hubbard W.B., Militzer B., Guillot T., Miguel Y., Movshovitz N., and Kaspi Y., et al. (2017) Comparing Jupiter interior structure models to Juno gravity measurements and the role of a dilute core. *Geophysical Research Letters* 44, 4649–4659. doi:10.1002/2017GL073160
- Wang, H.S., Lineweaver, C.H., and Ireland, T.R. (2018) The elemental abundances (with uncertainties) of the most Earth-like planet. *Icarus* 299, 460–474. doi:10.1016/j.icarus.2017.08.024
- Wang, H.S., Liu, F., Ireland, T.R., Brasser, R., Yong, D., and Lineweaver, C.H. (2019) Enhanced constraints on the interior composition and structure of terrestrial exoplanets. *Monthly Notices of the Royal Astronomical Society* 482, 2222–2233. doi:10.1093/mnras/sty2749
- Wolfgang, A. and Lopez, E. (2015) How Rocky Are They? The Composition Distribution of Kepler's Sub-Neptune Planet Candidates within 0.15 AU. *The Astrophysical Journal* 806, 183. doi:10.1088/0004-637X/806/2/183
- Yoffe G., Ofir A., Aharonson O., (2021) A Simplified Photodynamical Model for Planetary Mass Determination in Low-eccentricity Multitransiting Systems. *The Astrophysical Journal* 908, 114. doi:10.3847/1538-4357/abc87a
- Zeng, L. and Sasselov, D. (2013) A Detailed Model Grid for Solid Planets from 0.1 through 100 Earth Masses. *Publications of the Astronomical Society of the Pacific* 125, 227. doi:10.1086/669163
- Zeng, L., Sasselov, D.D., and Jacobsen, S.B. (2016) Mass-Radius Relation for Rocky Planets Based on PREM. *The Astrophysical Journal* 819, 127. doi:10.3847/0004-637X/819/2/127
- Zeng L., Jacobsen S.B., Sasselov D.D., Petaev M.I., Vanderburg A., Lopez-Morales M., and Perez-Mercader J., et al. (2019) Growth model interpretation of planet size distribution. *Proceedings of the National Academy of Science* 116, 9723–9728. doi:10.1073/pnas.1812905116

